Pharmacological Research 168 (2021) 105579

Contents lists available at ScienceDirect

Pharmacological Research

journal homepage: www.elsevier.com/locate/yphrs

Invited Review

Properties of FDA-approved small molecule phosphatidylinositol 3-kinase inhibitors prescribed for the treatment of malignancies

Robert Roskoski Jr.

Blue Ridge Institute for Medical Research, 3754 Brevard Road, Suite 116, Box 19, Horse Shoe, NC 28742-8814, United States

ARTICLE INFO

Keywords:
Breast cancer, chronic lymphocytic leukemia
Follicular lymphoma
Marginal zone lymphoma
PI 3-kinase structure
Small lymphocytic lymphoma

Chemical compounds studied in this article:
Acalabrutinib (PubChem CID: 71226662)
Alpelisib (PubChem CID: 56649450)
Copanlisib (PubChem CID: 135565596)
Duvelisib (PubChem CID: 50905713)
Fulvestrant (PubChem CID: 104741)
Ibrutinib (PubChem CID: 24821094)
Idelalisib (PubChem CID: 11625818)
Insulin (PubChem CID: 16131098)
Phosphatidylinositol-3,4,5-trisphosphate (PubChem CID: 53477782)
Umbralisib (PubChem CID: 72950888)

ABSTRACT

The discovery of the phosphatidylinositol 3-kinase (PI 3-kinase) pathway was a major advance in understanding eukaryotic signal transduction. The high frequency of PI 3-kinase pathway mutations in many cancers stimulated the development of drugs targeting these oncogenic mutants. The PI 3-kinases are divided into three classes and Class I PI 3-kinases, which catalyze the phosphorylation of phosphatidylinositol-4,5-bisphosphate (PI-4,5-P2) to generate phosphatidylinositol-3,4,5-trisphosphate (PIP3), are the main subject of this review. The class I PI 3-kinases are made up of p110α, p110β, p110δ, and p110γ catalytic subunits. These catalytic subunits are constitutively bound to regulatory subunits (p85α, p85β, p55γ, p101, and p87 proteins). The p85/p55 regulatory subunits heterodimerize with p110α or p110δ thereby forming complexes that are regulated chiefly by receptor protein-tyrosine kinases. The p101 and p87 subunits heterodimerize with p110γ to form complexes that are regulated mainly by G protein-coupled receptors (GPCRs). Complexes containing the p110β subunit are activated by receptor protein-tyrosine kinases as well as GPCRs. Following the generation of PIP3, the AKT and mTOR protein-serine/threonine kinases are activated leading to cell growth, proliferation, and survival. Like protein kinases, the PI 3-kinase domains consist of a bilobed structure connected by a hinge-linker segment. ATP and most PI 3-kinase and protein kinase inhibitors form hydrogen bonds with hinge residues. The small and large lobes of PI 3-kinases and protein kinases have a very similar three-dimensional structure called the protein kinase fold. Both PI 3-kinases and eukaryotic protein kinases possess an activation segment that begins with a DFG triad (Asp-Phe-Gly); the activation segment of protein kinases usually ends with an APE (Ala-Pro-Glu) signature while that of PI 3-kinases ends with a PFxLT (Pro-Phe-Xxx-Leu-Thr) signature. Dormant PI 3-kinases have a collapsed activation loop and active PI 3-kinases have an extended activation loop. The distance between the α-carbon atom of the DFG-D residue at the beginning of the activation loop and that of the PFxLT-F residue at the end of the activation loop in dormant PI 3-kinases is about 13 Å; this distance in active PI 3-kinases is about 18 Å. The protein kinase catalytic loop has an HRD (His-Arg-Asp) signature while that of the PI 3-kinases reverses the order with a DRH triad. Alpelisib is an orally effective FDA-approved PI 3-kinase-α inhibitor used for the treatment of breast cancer. Copanlisib, duvelisib, idelalisib, and umbralisib are PI 3-kinase-δ inhibitors that are approved for the third-line treatment of follicular lymphomas and other hematological disorders. Copanlisib is also a potent inhibitor of PI 3-kinase-α. Of the five approved drugs, all are orally bioavailable except copanlisib. Idelalisib interacts with the active conformation of PI 3-kinase-δ and is classified as a type I inhibitor. Alpelisib and copanlisib interact with inactive PI 3-kinase-α and PI 3-kinase-γ, respectively, and are classified as a type I½ antagonists. Except for umbralisib with a molecular weight of 571.5, all five drugs conform to the Lipinski rule of five for oral effectiveness. Copanlisib, however, must be given intravenously. Alpelisib and copanlisib inhibit PI 3-kinase-α, which is involved in insulin signaling, and both drugs promote insulin-resistance and produce hyperglycemia. The five FDA-approved PI 3-kinase inhibitors produce significant on-target toxicities, more so than

Abbreviations: aPKs, atypical protein kinases; AS, activation segment; BTK, Bruton protein-tyrosine kinase; Cat D, catalytic domain; CLL, chronic lymphocytic leukemia; CS or C-spine, catalytic spine; CL, catalytic loop; EGFR, epidermal growth factor receptor; ePKs, eukaryotic protein kinases; FL, follicular lymphoma; GK, gatekeeper; GPCR, G protein-coupled receptor; GRL, Gly-rich loop; IP3, inositol trisphosphate; MZL, marginal zone lymphoma; PDGFR, platelet-derived growth factor receptor; PI, phosphatidylinositol; PIK3CA, phosphatidylinositol 3-kinase catalytic subunit-α; PI3K, phosphatidylinositol 3-kinase; PI-4, 5-P2 or PIP2, phosphatidylinositol-4,5-bisphosphate; PIP3, phosphatidylinositol-3,4,5-trisphosphate; PKA, protein kinase A; PKC, protein kinase C; pY, phosphotyrosine; RS or R-spine, regulatory spine; Sh2, shell residue 2; SLL, small lymphocytic lymphoma; VEGFR, vascular endothelial growth factor receptor.

E-mail address: rrj@brimr.org.

https://doi.org/10.1016/j.phrs.2021.105579
Received 22 March 2021; Accepted 22 March 2021
Available online 26 March 2021

many approved protein kinase antagonists. The development of PI 3-kinase inhibitors with fewer toxicities is an important long-term therapeutic goal.

1. Overview of phosphatidylinositol 3-kinases and their signaling pathways

Cell growth and proliferation in mammals are regulated by signals initiated by numerous growth factors [1–3]. Such signals are transduced across the plasma membrane through protein-tyrosine kinase receptors such as the epidermal growth factor receptors [4–7], the fibroblast growth factor receptors [8], the platelet-derived growth factor receptors [9], the Kit stem cell factor receptor [10–12], the RET glial-cell derived receptor [13], the ROS1 orphan receptor [14], and the vascular endothelial growth factor receptors [15–17]. The receptors activate intracellular signaling through the phosphatidylinositol 3-kinase (PI 3-kinase) pathway and the Ras-Raf-MEK-ERK MAP kinase pathways [18]. In addition to growth factor receptors, the PI 3-kinase pathway is activated by the B-cell receptor and G-protein-coupled receptors (GPCRs) [19–21]. A simplified diagram that covers the main branches of the MAP kinase and PI 3-kinase signaling pathways is provided in Fig. 1.

PI 3-kinase catalyzes the phosphorylation of phosphatidylinositol-4,5-bisphosphate (PI-4,5-P2) to generate phosphatidylinositol-3,4,5-trisphosphate (PIP3). Phosphatidylinositols are lipids made up of two acyl chains covalently linked to glycerol (making diacylglycerol) that is fused to the six-carbon myo-inositol headgroup as a phosphodiester. This headgroup bears hydroxyl groups at the 2-, 3-, 4-, 5-, and 6-positions; the 3-, 4- and 5-hydroxyl groups can be phosphorylated and the location of phosphates determines how the phosphoinositide interacts with proteins [3]. PI 3-kinase is a generic term for the lipid kinases that catalyze the phosphorylation of a phosphoinositide at the 3-position according to the following chemical equation:

$$\text{PI-4,5-P2} + \text{ATP} \rightarrow \text{PI-3,4,5-P3} + \text{ADP}$$

The PI 3-kinases are divided into three classes: class I PI 3-kinases mediate the conversion of PI-4,5-P2 to PIP3 and include the isoforms that are most frequently mutated in cancer. These are the main subject of this review. The class II PI 3-kinases catalyze the conversion of PI-4-P to PI-3,4-P2; this important signaling phospholipid occurs on early endosomes and participates in protein kinase AKT signaling [18,22]. Class III PI 3-kinases mediate the conversion of PI to PI-3-P, a major phospholipid that participates in autophagy and vesicular trafficking [23–25]. The class III Vps34 was first identified in *Saccharomyces cerevisiae* (budding yeast) as a protein involved vesicle-mediated Vacuolar protein sorting (Vps) and *vps34* refers to a complementation group name. Table 1 summarizes the properties of the three classes of PI 3-kinases.

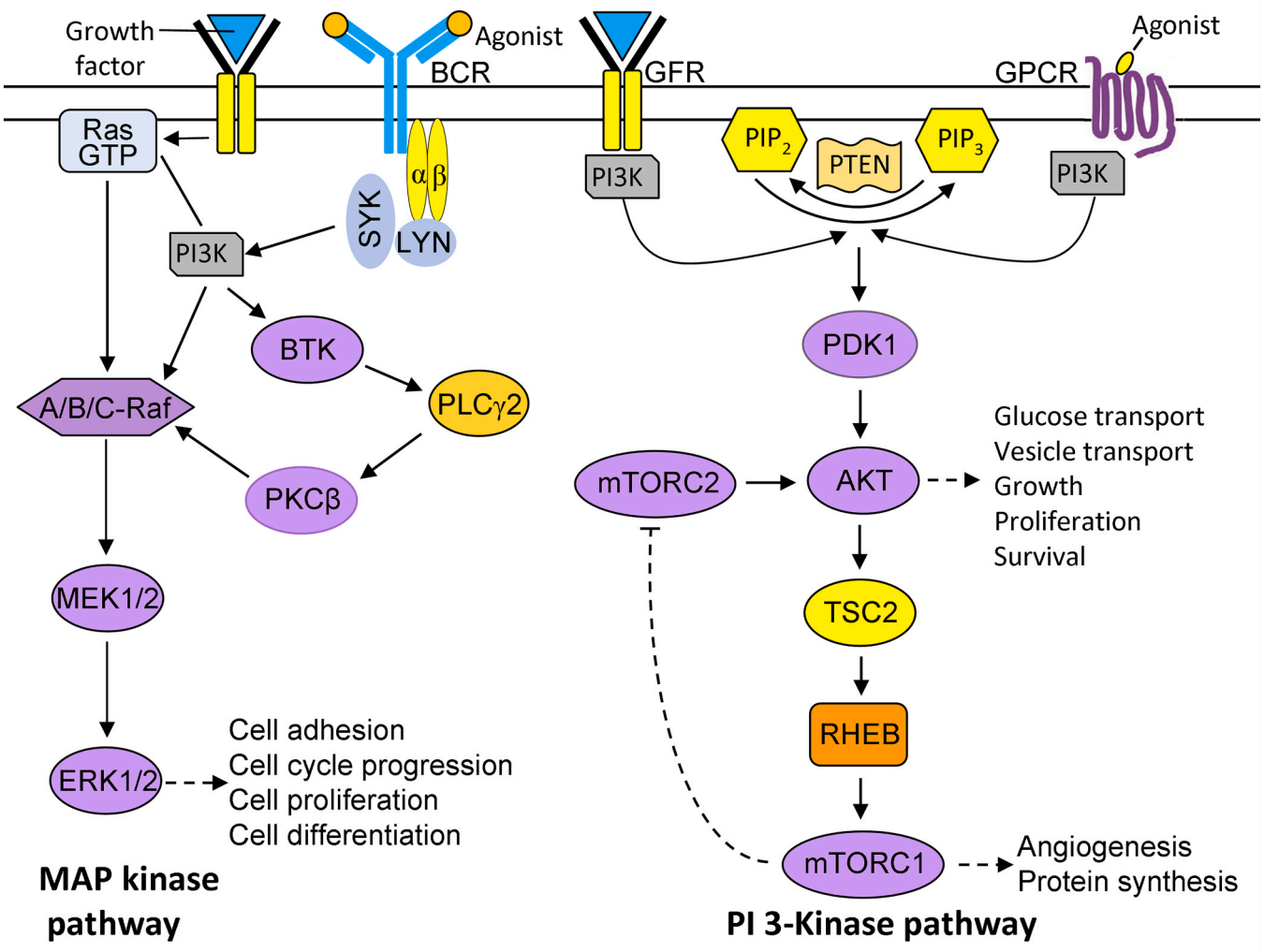

Fig. 1. MAP kinase and PI 3-kinase signaling pathways. BCR, B-cell receptor; GFR, growth factor receptor; GPCR, G protein-coupled receptor.

Table 1
Classes of PI 3-kinases.[a]

PI3K Classes	Catalytic subunits (*gene*) tissue distribution	Regulatory subunits (*gene*)
Class I		
IA	p110α (*PIK3CA*) ubiquitous p110β (*PIK3CB*) ubiquitous p110δ (*PIK3CD*) hematopoietic	p85α (*PIK3R1*) p55α (*PIK3R1*) p50α (*PIK3R1*) p85β (*PIK3R2*) p55γ (*PIK3R3*)
IB	p110γ (*PIK3CG*) hematopoietic	p101 (*PIK3R5*) p84 (*PIK3R6*)
Class II		
II	PI3KC2α (*PIK3C2A*) ubiquitous PI3KC2β (*PIK3C2B*) ubiquitous PI3KC2γ (*PIK3C2G*) gastrointestinal tract and liver	None
Class III		
Complex I	VPS34 (*PIK3C3*) ubiquitous	Beclin I (*BECN1*) PIK3R4 (*PIK3R4*) ATG14 (*ATG14*)
Complex II	VPS34 (*PIK3C3*) ubiquitous	Beclin I (*BECN1*) PIK3R4 (*PIK3R4*) UVRAG (*UVRAG*)

[a] Adapted from Ref. [25].

The class I PI 3-kinases are made up of catalytic subunits (p110) that correspond to four genes (*PIK3CA*, *PIK3CB*, *PIK3CD*, and *PIK3CG*) that encode the p110α, p110β, p110δ, and p110γ isoforms, respectively [25]. These catalytic subunits are constitutively bound to regulatory subunits that correspond to five genes (*PIK3R1*, *PIK3R2*, *PIK3R3*, *PIK3R5*, and *PIK3R6*) that encode, respectively, the p85α, p85β, p55γ, p101, and p87 proteins (Fig. 2). The p85/p55 regulatory subunits heterodimerize with p110α or p110δ thereby forming complexes that are regulated chiefly by receptor tyrosine kinases. The p101 and p87 subunits heterodimerize with p110γ to form complexes that are regulated mainly by G protein-coupled receptors (GPCRs). Complexes containing the p110β subunit are activated by receptor tyrosine kinases as well as GPCRs. The p85/p55 regulatory subunits contain an N-terminal SH2 domain (nSH2), a C-terminal SH2 domain (cSH2), and an inter-SH2 (iSH2) coiled-coil domain that mediates the interaction with the various catalytic subunits. The SH2 domains bind to pYxxM amino acid motifs of activated receptor protein-tyrosine kinases or their adapter proteins that result in the recruitment of PI 3-kinases to the plasma membrane where their substrate (PI-4,5-P2) is abundant and triggers conformational changes that enhance PI 3-kinase catalytic activity [26,27].

PIK3CA and PIK3CB occur in all tissue types while PIK3CD and PIK3CG are found more generally in hematopoietic and immune cells (the C denotes catalytic and the A/B/D/G refer to the specific forms as α, β, δ, γ) [25]. Following the activation of a receptor protein-tyrosine kinase by its growth factor, the activated receptor or its adapter proteins undergo tyrosine phosphorylation on multiple YxxM motifs that in turn interact with the SH2 domains of the p85 regulatory subunit to change the PI 3-kinase catalytic subunit conformation while attracting it to the substrate-rich plasma membrane, thereby resulting in the biosynthesis of PIP3 [1]. Additionally, protein kinase AKT is activated following its binding to PIP3 within the plasma membrane and thus mediates downstream growth and survival pathways (Fig. 1). The PIP3 signal is terminated by the action of phosphatases. PIP3 is converted to PI-4,5-P2 following the hydrolysis catalyzed by PTEN (phosphatase and tensin

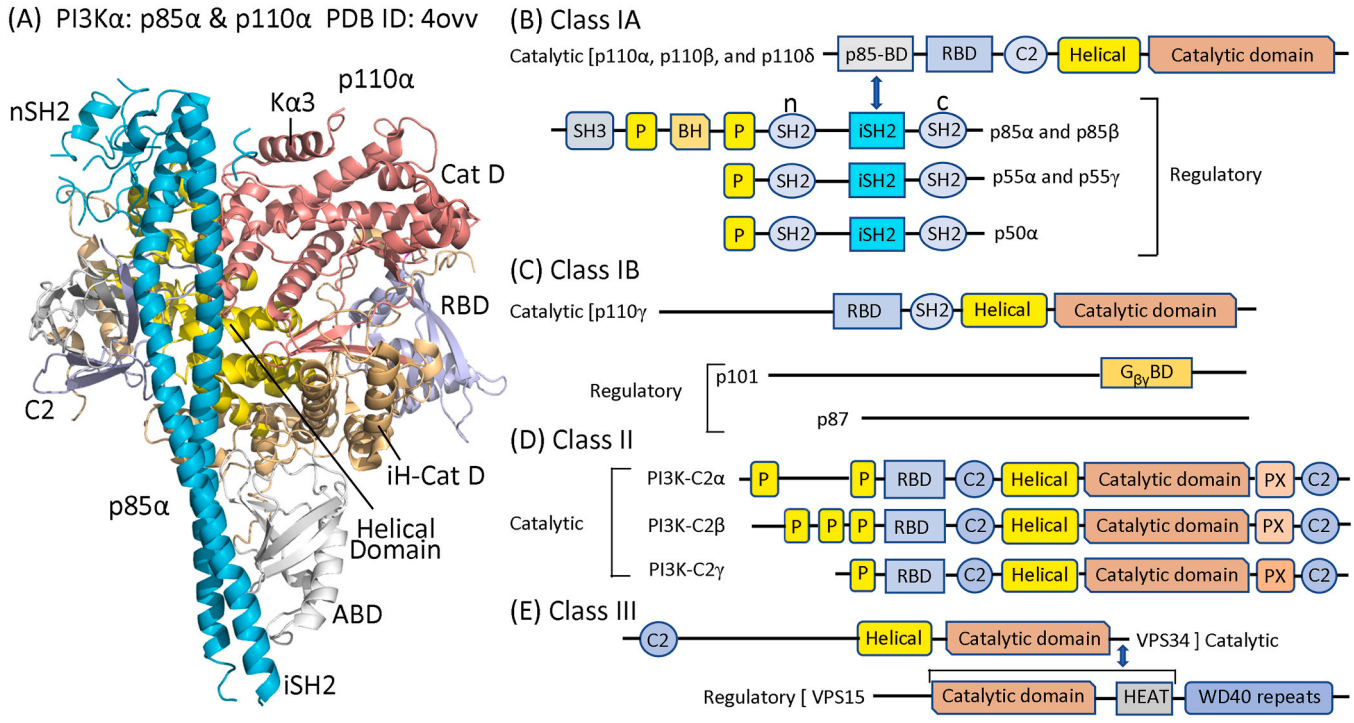

Fig. 2. Structure and organization of the PI 3-kinase family. (A) p110α secondary and tertiary structure. A portion of the regulatory domain (p85α) is depicted in cyan. iH-Cat D, interhelical-catalytic domain. (B) Class IA enzymes are heterodimers of a p110 catalytic subunit and a p85-type of regulatory subunit; the three regulatory isoforms result from the alternative splicing of pre-mRNA. Class IA catalytic isoforms have a p85-binding domain (p85-BD), a Ras-binding domain (RBD), a C2 membrane-interacting domain, a helical domain, and a catalytic domain. Class IA p85 regulatory isoforms have an inter-SH2 (iSH2) domain that binds to the Class IA catalytic subunit; it is flanked by SH2 domains that bind to pYxxM motifs. The longer isoforms have an amino-terminal SH3 and breakpoint cluster homology (BH) domains. (C) Class IB PK3Ks are heterodimers of a p110γ catalytic subunit and a p101 or p87 regulatory subunit. The p101 regulatory subunit binds to G-protein $G_{\beta\gamma}$ subunits. (D) Class II isoforms function as monomers. (E) VPS34 makes up the Class III catalytic subunit. It forms a constitutive heterodimer with the myristoylated, membrane-associated VPS15 protein. ABD, adapter binding domain; BH, breakpoint cluster homology domain; C2, membrane-interacting domain; iSH2, inter-SH2 domain; P, proline-rich domain; PX, Phox homology domain; RBD, Ras binding domain. Adapted from Ref. [1]. Section A and Figs. 3, 4, and 8 were prepared using the PyMOL Molecular Graphics System Version 1.5.0.4 Schrödinger, LLC.

homolog) or it is converted to PI-3,4-P2 in a reaction catalyzed by Ship2 (phosphatidyl-3,4,5-trisphosphate 5-phosphatase) [28].

CXCR4, a member of the family of chemokine-activated G protein-coupled receptors, is widely expressed in immune response cells. It is involved in both cancer development and progression and is implicated in the pathophysiology of chronic lymphocytic leukemia and small lymphocytic lymphoma [29]. Moreover, many cancer cells express higher levels of CXCR4 when compared with their normal cellular counterparts. Activation of PI 3-kinase by G protein-coupled receptors such as CXCR4 is mediated by the Gβ/γ subunit that can bind and activate both p110β and p110γ [25]. The activation of AKT by CXCR4 follows the stimulation of p110β and p110γ activity.

The PIP3 generated by the action of PI 3-kinase binds to the PH (pleckstrin homology) domain of AKT/PKB and attracts it to the plasma membrane [1–3]. AKT is activated following its phosphorylation catalyzed by PDK1 (phosphoinositide-dependent protein kinase-1) and mTORC2 (mammalian target of rapamycin complex-2); all three of these enzymes are protein-serine/threonine kinases. AKT catalyzes the phosphorylation and inhibition of glycogen synthase kinase-3 (GSK3). AKT also regulates the activity of TSC2 (tuberous sclerosis complex-2) and RHEB leading to the activation of mTORC1, which participates in the regulation of ribosomal S6 kinase (S6K) and the 4E-BP transcription factor. As a result, the action of AKT promotes cell growth, proliferation, survival and protein synthesis and angiogenesis (Fig. 1). Importantly, mTORC1 functions as a negative feedback inhibitor of mTORC2C. PI 3-kinase activation initiates a cascade of downstream signals that promotes glucose uptake via GLUT1, cell growth mediated by the mTOR complex 1 (mTORC1) containing the mammalian target of rapamycin protein kinase (mTOR), and cell survival [3]. Owing to its pivotal role in cell division, survival, and metabolism, there has been considerable interest and work in targeting the PI 3-kinase pathway with novel pharmaceuticals.

The development and activation of immune B-cells is dependent upon the PI 3-kinase pathway involving the p110δ and p110γ isoforms, which are predominately expressed in hematopoietic cells [25]. During B-cell development, the immunoglobulin variable (V), diversity (D), and junction genes (J) are recombined to generate a unique sequence that produces the B-cell receptor antigen-binding site [30]. B-cell receptor signaling requires an intricate network of adapters and protein kinases that convert antigen stimulation to intracellular responses. The B-cell receptor complex is made up of the receptor bound to a disulfide-linked Igα-Igβ heterodimer as depicted in Fig. 1. After antigen stimulation of the receptor, the Src family kinase Lyn catalyzes the phosphorylation of pairs of tyrosine residues in Igα-Igβ immunoreceptor tyrosine-based activation motifs (ITAMs) thereby creating a docking site for the two SH2 domains of spleen protein-tyrosine kinase (SYK) [31]. SYK then attracts and activates PI3Kδ, which catalyzes the conversion of membrane-bound PI-4,5-P2 to PIP3. The N-terminal PH lipid-interaction module of BTK is attracted to PIP3 that stimulates SYK and Lyn to catalyze the *trans*-phosphorylation of BTK at Tyr551 within the activation segment that produces an active enzyme. The attraction of BTK dimers to membrane-bound PIP3 can also produce activation segment *trans*-autophosphorylation and activation.

BTK catalyzes the phosphorylation of PLCγ2 at two residues (Y753 and Y759) producing an increase in phospholipase enzyme activity [32]. PLCγ2 catalyzes the hydrolysis of PI-4,5-P2 to generate inositol trisphosphate (IP3) and diacylglycerol (DAG). IP3 action releases Ca^{2+} from intracellular stores that activate PLCγ2. In turn, DAG and Ca^{2+} activate PKCβ, which leads to the activation of the Ras/Raf/MEK/ERK signaling module that promotes cell growth and proliferation [33–38]. SYK is also activated by the B-cell receptor leading to the phosphorylation of c-Cbl, which provides docking sites for the SH2 domain of the p85 regulatory subunit of PI3Kα and subsequent activation of the catalytic subunit. The PI 3-kinase-mediated module downstream of the B-cell receptor is necessary and sufficient for B-cell survival and represents a key pathway for the pathogenesis of B-cell lymphoproliferative diseases including follicular lymphomas and chronic lymphocytic leukemias. PI3Kδ mediates B-cell receptor-driven chemotaxis and proliferation and PI3Kγ is an important component of diverse immune processes including T-cell functioning [29,39].

The PI 3-kinase and MAP kinase signaling modules are among the most important oncogenic drivers of human malignancies [1–3,20,32,40]. These evolutionarily conserved pathways relay extracellular signals to intracellular signaling cascades. Like the PI 3-kinase pathway, the MAP kinase pathway is activated by the same transmembrane receptors. For example, activated EGFR becomes auto-phosphorylated at tyrosine residues that interact with guanine nucleotide exchange factors (GEFs) such as SOS (from *Drosophila* son of sevenless) as well as other adapter proteins. These factors facilitate the conversion of dormant Ras-GDP to the functional Ras-GTP in the plasma membrane [41–43]. These Ras proteins toggle between dormant and active forms; the conversion of inactive Ras-GDP to active Ras-GTP turns the switch on and the intrinsic Ras-GTPase activity stimulated by the GTPase activating proteins (GAPs) such as NF1 (neurofibromin-1) turns the switch off. Note that much of PI 3-kinase and Ras biochemistry and signaling occur within the inner leaflet of the plasma membrane.

To activate the MAP kinase module, Ras-GTP stimulates the formation of active homodimers or heterodimers made up of A/B/C-Raf by an intricate process (the Raf acronym corresponds to *R*apidly *a*ccelerated *f*ibrosarcoma, first described in mice). The Raf family of enzymes are protein-serine/threonine protein kinases that catalyze the phosphorylation and activation of MEK1 and MEK2 (*M*AP/*E*RK *K*inase). The MEK protein kinases, in turn, catalyze the phosphorylation and activation of ERK1 and ERK2 (*E*xtracellular Signal-*R*egulated protein *K*inases). The A/B/C-Raf enzymes and MEK1/2 have very narrow substrate specificity [37,38]. Accordingly, the only known Raf substrates are MEK1/2 and the only known MEK1/2 substrates are ERK1/2. In contrast to these enzyme families, ERK1/2 have broad substrate specificity and they catalyze the phosphorylation of hundreds of different cytosolic and nuclear proteins. The linear MAP kinase pathway branches extensively at the ERK1/2 node. The existence of parallel pathways downstream from activated receptors and oncogenes suggests a strategy of combining targeted inhibitors of Raf, MEK, or ERK of the MAP kinase pathway along with inhibition of PI 3-kinase, PKB/AKT, or mTOR of the PI3K pathway in the treatment of various neoplasms [44].

Mutations involving the PI 3-kinase pathway are among the most common mutations involved in the pathogenesis of cancer [40]. *PIK3CA* is the second most highly mutated protein in cancer following only p53 [45]. Zhang et al. reported that *PIK3CA* was mutated in 14% of all cancers and amplified in 6% of all cancers in their pan-cancer proteogenomic atlas [46]. They also reported that *PTEN* mutations occurred in 9% of all cancers in their data base. PI 3-kinase mutations and overexpression that increase enzyme activity promote cell growth and proliferation independently of growth factors and their receptors and result in neoplastic transformation. Mutations of *PIK3CA*, *PIK3R1*, *PTEN*, and *AKT* together occur in about one-third of all solid tumors. Besides the high incidence of cancers with mutations involving the PI 3-kinase pathway, increased PI 3-kinase activity has been linked to promoting signals from other driver mutations including those of *RAS* [41–43] and *ERBB2/HER2* [6,7].

PI 3-kinase activation has been implicated as a mechanism of tumor escape from HER2-targeted therapies and the combined inhibition of PI 3-kinase and HER2 has improved efficacy in preclinical studies leading to clinical trials with combination therapy [47]. The most common PI 3-kinase pathway mutations in cancers occur in *PIK3CA*, which encodes p110α [45]. This isoform is chiefly responsible for mediating signaling by receptor protein-tyrosine kinases, making p110α an attractive therapeutic target. The importance of the PI 3-kinase signaling pathway in many cell types is underscored by the toxicities observed clinically following the use of PI3K-p110α-specific inhibitors. An ideal drug would inhibit the mutant protein and promote maximal cancer-specific benefits, while at the same time avoiding general toxicities [3].

2. Comparison of phosphatidylinositol 3-kinases and eukaryotic protein kinases

The 555 members of the human protein kinase superfamily consist of a main class of 497 eukaryotic protein kinases (ePKs) and a second class of 58 atypical protein kinases (aPKs), which include the PI 3-kinases [48]. The class I and class III PI 3-kinases consist of both regulatory and catalytic subunits whereas the class II enzymes consist of only a catalytic subunit. Nearly all of the regulatory and catalytic subunits contain various structural and functional domains (Fig. 2). The 1068-residue PI3Kα catalytic domain contains (from the N- to C-terminus) a p85-binding domain (p85-BD), a Ras-binding domain (RBD), a C2 membrane-interacting domain, a helical domain, and an N-terminal catalytic domain (Fig. 2). The catalytic domain of the PI 3-kinases share the prototypical structural eukaryotic protein kinase (ePK) fold (Fig. 3) despite a lack of sequence similarity. The PI 3-kinase catalytic domain consists of a small amino-terminal lobe and a larger carboxyterminal lobe with an ATP-binding cleft between them. Like protein kinases, the small PI 3-kinase lobe usually contains five β-sheets and an α-helix (Kα3 in PI 3-kinases and αC in ePKs).

In eukaryotic protein kinases, the αC-helix plays an important regulatory role existing in an active αC_{in} and inactive αC_{out} conformation [49]. In the αC_{in} conformation, there is a salt bridge from a conserved glutamate in the αC-helix to a β3-AxK-lysine; this salt bridge is absent in the αC_{out} conformation. PI 3-kinases contain an aspartate instead of a glutamate at a comparable position; however, this residue is too short to make contact with a corresponding lysine residue. In contrast to eukaryotic protein kinases, the overall structure of the small lobe of PI 3-kinases varies little, if at all, with the activation state. The loop connecting the β1- and β2-helices interacts with the ATP phosphates. In protein kinases it is called the G-rich loop and consists of a GxGxØG sequence (Ø represents a hydrophobic amino acid such as phenylalanine). This component is called the P-loop in PI 3-kinases because its sequence is not G-rich. In PI3Kα, the P-loop (MSSAKR) contains no glycine residues.

Both PI 3-kinases and ePKs contain a hinge-linker that connects the small and large lobes and the hinge of each forms hydrogen bonds with ATP [48,50]. Both ePKs and PI 3-kinases contain an αD- and αE-helix in the large lobe. In contrast to ePKs, PI 3-kinases lack a helix that corresponds to the αF-helix. The large lobe of PI 3-kinases, however, contains Kα4/5/6/7/8/9/10/11/12-helices. Kα4 and Kα5 correspond to the ePK αD- and αE-helices. ePKs contain a catalytic loop that begins with HRD; the PI 3-kinase catalytic loop has a mirrored sequence of DRH. The HRD-aspartate of ePKs functions as a catalytic base by abstracting a proton from the substrate during its attack on the γ-phosphate of ATP [49].

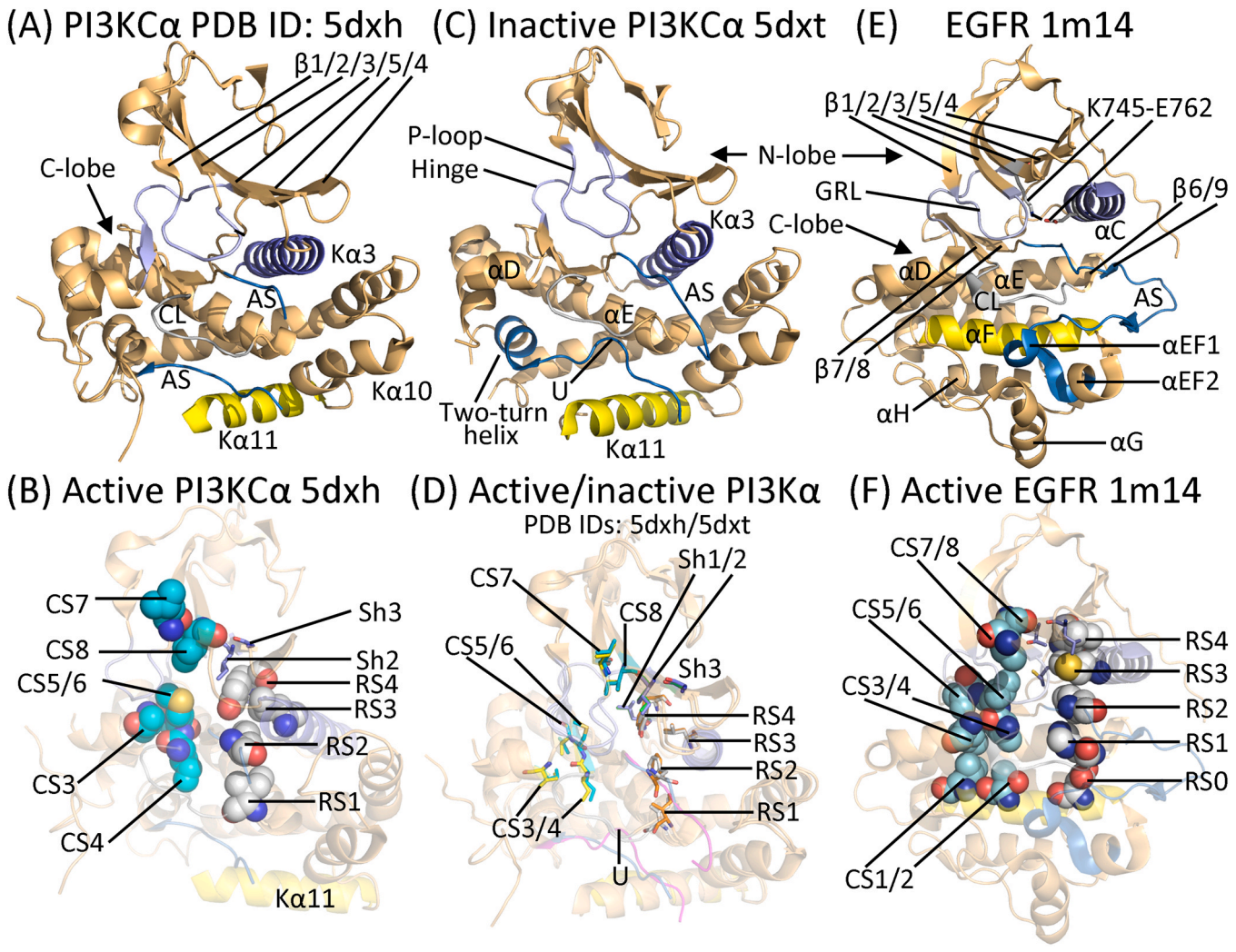

Fig. 3. Overview of the structure of PI 3-kinases and EGFR. (A) Active PI3Kα. (B) Spine and shell residues of active PI3Kα. (C) Inactive PI3Kα. (D) Superposition of the spine and shell residues of active and inactive PI3Kα. (E) Overview of the structure of active EGFR. (F) Spine and shell residues of active EGFR. The dash in (E) depicts a polar bond. AS, activation segment; CL, catalytic loop; CS, catalytic spine; Sh, Shell; U is the U-shaped end of the activation segment of an inactive PI 3-kinase.

Both PI 3-kinases and ePKs contain an activation segment that begins with a DFG canonical sequence [48]. The activation segments present their respective substrates to ATP during catalysis. The ePK activation segments are 35–40 residues long and they usually, but not always, end with an APE sequence [49]. The PI 3-kinase activation segments are shorter (about 25 residues long) and they end with a PFxLT sequence [48]. The PI 3-kinase activation loop possesses a first basic box (xKxK) that interacts with the phosphates of the PI-4,5-P2 substrate [51]. The activation segment of ePKs exists in an inactive closed conformation and an active open conformation. The ePK active conformation is generally stabilized following the phosphorylation of activation segment residues (serine/threonine or tyrosine, depending upon the class of the protein kinase). In marked contrast, there is no evidence that the PI 3-kinase activation segment undergoes regulatory phosphorylation [50]. The PFxLT sequence of PI 3-kinases is often contained within a short two-turn helix (Fig. 3C).

Like ePKs, the activation segment of PI 3-kinases exists in an active and inactive conformation. The analysis of Zhang et al. indicates that the nSH2 domain of the regulatory subunit is a critical component in the control of class IA PI 3-kinase catalytic activity by its interaction with the activation loop [51]. The negatively charged acidic motif of nSH2 interacts with the second basic box (KRER) of the activation segment and confines the activation loop in a closed or collapsed conformation. When nSH2 domains interact with growth factor receptors or their adapter proteins containing phosphotyrosines, the activation loop is freed from the nSH2 domain and the loop becomes extended. The activation segment of dormant PI 3-kinases possesses a U-shaped conformation at its end that interacts with the Kα11-helix with an "in" conformation (Fig. 3C). The activation segment of a functional enzyme lacks the U conformation with a $K\alpha11_{out}$ structure. The distance between the α-carbon atom of the DFG-D residue and that of the α-carbon atom of the PFxLT-F residue for PI 3-kinases with a collapsed activation loop is about 13 Å and this distance in PI 3-kinases with an extended activation loop is about 18 Å. Overall changes in the structure of the large lobe of PI 3-kinases reflect the active and inactive states whereas the conformation of the small lobe is the same in both states.

The PI 3-kinases contain an adenine-binding pocket, a specificity pocket, and an affinity pocket [50,52]. As in the case of ePKs, most drugs that target PI 3-kinases interact with the adenine pocket and form hydrogen bonds with the hinge. Studies with PIK-39, a quinazolinone-purine PI 3-kinase inhibitor similar to idelalisib, indicated that it produced a conformational rearrangement of a conserved methionine residue (M752 in p110δ) that induces the creation of a so-called "specificity pocket" in the ATP-binding site between this residue and a conserved tryptophan (W760 in p110δ). These and other p110δ-selective compounds with their quinazolinone moiety fit snugly into this newly formed hydrophobic pocket. The gatekeeper residue of PI 3-kinases is an isoleucine residue that forms part of the wall of a very small hydrophobic region. Many PI3K inhibitors occupy this space, which is called the "affinity pocket." Table 2 provides a summary of important residues found in human PI 3-kinases and EGFR.

Kornev et al. described eight hydrophobic residues in protein kinases that form a catalytic or C-spine and four hydrophobic residues that form a regulatory or R-spine [53,54]. Both spines contain amino acid residues from both the small and large lobes. The R-spine contains one residue from the regulatory αC-helix and another from the activation segment (DFG-F), both of which are major regulatory components that assume active and inactive conformations. The bottom of the R-spine within the large lobe anchors the catalytic loop and activation segment in an active state and the C-spine positions ATP in the active site thereby promoting catalysis. Moreover, the proper alignment of each spine is required for the assembly of an active enzyme as shown for the EGFR in Fig. 3F. In the inactive αC_{out} structure, residue RS3 is displaced outwardly; in the protein kinase DFG-D_{out} conformation RS2 is displaced inwardly and the R-spine is broken (See Ref. [49] for further information and structures).

In contrast to the protein kinases, the catalytic and regulatory spines of active and inactive PI 3-kinases are nearly superimposable (Fig. 3D). The main structural differences between active and dormant PI 3-kinases reside at the end of the activation segment and in the position of the Kα11-helix [51]. Neither of these components contain C-spine or

Table 2
Important residues in the human PI 3-kinases and EGFR.

Protein kinase[a]	PI3Kα	PI3Kβ	PI3Kδ	PI3Kγ	EGFR	Inferred function
Kinase domain	797–1068	800–1067	774–1041	828–1073	712–979	Catalyzes substrate phosphorylation
P-loop or GRL	^{772}MSSAKR^{777}	^{779}MDSKMK^{784}	^{752}MDSKMK^{757}	^{804}MASKKK^{809}	^{719} GSGAFG^{724}	Anchors ATP α- and β-phosphates
β3-strand lysine	K802	K805	K779	K833	K745	Forms salt bridges with ATP α- and β-phosphates
The Kα3-D or αC-E	D806	D809	D783	D837	E762	Forms salt bridges with β3-K in ePKs only
Hinge residues	^{849}EVV^{851}	^{852}EVV^{854}	^{826}EVV^{828}	^{880}EIV^{882}	^{791}QLM^{793}	Forms H-bonds with ATP-adenine
Gatekeeper residue	I848	I851	I825	I879	T790	Limits access to the back pocket
CL	^{913}IGDRHNSN^{920}	^{917}IGDRHSDN^{924}	^{891}IGDRHSDN^{898}	^{944}IGDRHNDN^{951}	^{835}HRDLAARN^{842}	Plays both structural and catalytic roles
CL His	917	921	895	948	835	Interacts with ATP γ-phosphate in PI3Ks only
CL Asn	920	924	898	951	842	Binds Mg^{2+} (2)
Beginning DFG of AS	933–935	937–939	911–913	964–966	855–857	Participates in the regulation of the active state
End of AS	^{953}PFVLT^{957}	^{957}PFILT^{961}	^{931}PFILT^{935}	^{984}PFVLT^{988}	^{882}ALE^{884}	
AS D	933D	937D	911D	964D	855D	Binds Mg^{2+} (1)
Adenine pocket	I800, Y836, F930, M922	I803, Y839, M926, F935	I777, Y813, M900, F908	I831, Y867, M953, F961	L718, A743, L792, M793, L844	Interacts with adenine
Affinity pocket	Y836, I848, I932, D810	Y839, I851, I936, D813	Y813, I825, I910, D787	Y867, I879, I963, D841	None	Small hydrophobic pocket adjacent to the gatekeeper in PI3Ks
Specificity pocket	M772, W780	M779, W787	M752, W760	M804, W812	None	Induced by some PI3K inhibitors
No. of residues	1068	1070	1044	1102	1210	
Molecular Weight (kDa)	124.3	122.8	119.5	126.5	134.3	
UniProtKB accession no.	P42336	P42338	O00329	P48736	P00533	

[a] AS, Activation Segment; CL, Catalytic Loop; GRL, glycine-rich loop.

R-spine residues so that it is not surprising that the three-dimensional location of these spines do not differ between active and inactive PI 3-kinase conformations.

Based upon site-directed mutagenesis studies, Meharena et al. defined three shell (Sh) residues in the PKA catalytic subunit that support the R-spine, which they called Sh1, Sh2, and Sh3 [55]. The Sh2 residue represents the protein kinase gatekeeper residue. This residue plays a critical role in controlling access to hydrophobic pocket II (HPII) or the back pocket of protein kinases. In contrast to the identification of the HRD, DRH, and DFG signatures, which are related to the amino acid sequence, the two spines were identified by their three-dimensional location in inactive or active protein kinases [53,54]. Table 3 provides a compilation of the spine and shell residues of select PI 3-kinases and human EGFR. Small molecule protein kinase inhibitors regularly interact with residues within the R-spine, C-spine, and shell residues [56–58] and PI 3-kinase antagonists possess this property as described in Section 5.

Most PI 3-kinase and protein kinase antagonists bind within the ATP-binding site in the cleft that separates the small and large kinase lobes [48]. The exocyclic amino group of ATP characteristically interacts with a carbonyl group of the first hinge residue of PI 3-kinases and protein kinases. The hinge-linker residues follow the β5-strand and connect the amino-terminal and carboxyterminal lobes. For EGFR/ErbB1, the 6-amino group of the adenine base of ATP forms a hydrogen bond with the carbonyl oxygen of Q791 (PDB ID: 2GS6), the first hinge residue of EGFR. The adenine *N*1 nitrogen forms a hydrogen bond with the –NH group of M793, the third hinge residue. The ATP α-phosphate group binds to the invariant AxK-K745 of the β3-strand, which in turn makes a salt bridge with conserved E762 of the αC-helix (Fig. 4A). Furthermore, the ATP γ-phosphoryl group forms a salt bridge with Mg^{2+}(1), which in turn binds to DFG-D854 (not shown).

ATP binds to PI 3-kinase in a similar fashion. The 6-amino group and purine base of ATP form hydrogen bonds with the first and third hinge residues and the α-phosphate forms a salt bridge with a β3-strand K776 (Fig. 4B). DFG-D933 interacts with Mg^{2+} (1), which then interacts with the β- and γ-phosphates. The asparagine at the end of the catalytic loop (N920) interacts with Mg^{2+} (2) that then interacts with the β- and γ-phosphates (not shown) [59]. H936 within the activation segment acts as a Lowry–Bronsted base (proton acceptor) to remove the proton from the 3′ –OH group of the PIP2 substrate [59]. DRH-H917 of the catalytic loop binds to the ATP γ-phosphate. In ePKs, it is the HRD-aspartate that functions as a base to remove the proton from the protein substrate [49]. Assuming that the molecular weight of PIK3CA is 124.3 kDa and that of PIK3R1 is 83.6 kDa, the k_{cat} for PI3Kα is 7.08/min (1.7 pmol/min/50 ng of enzyme) with ATP and diC8-PIP2 as substrates as reported by Maheshwari et al. [59]. These investigators found that the K_m values for ATP and diC8-PIP2 were 2.00 μM and 1.80 μM, respectively. Structural studies indicate that the adenine moiety extends to the β2-strand, but

Table 3
Spine and shell residues in selected PI 3-kinases and human EGFR.

	Symbol	KLIFS No.[a]	Human PI3Kα	Human PI3Kγ	Murine PI3Kδ	Human EGFR
Regulatory spine						
β4-strand (N-lobe)	RS4	38	Y836	Y867	Y813	L777
C-helix (N-lobe)	RS3	28	L814	L845	L791	M766
Activation loop F of DFG (C-lobe)	RS2	82	F934	F965	F912	F856
Catalytic loop I/H (C-lobe)	RS1	68	I913	I944	I891	H835
F-helix (C-lobe)	RS0	None	None	None	None	D896
R-shell						
Two residues upstream from the gatekeeper	Sh3	43	G846	G877	G823	L788
Gatekeeper, end of β5-strand	Sh2	45	I848	I879	I825	T790
αC-β4 loop	Sh1	36	L834	L865	T811	C775
Catalytic spine						
β3-I/AxK motif (N-lobe)	CS8	15	I800	I831	I777	A743
β2-strand (N-lobe)	CS7	11	L779	L811	L759	V726
β7-strand (C-lobe)	CS6	77	M922	M953	M900	L844
β7-strand (C-lobe)	CS5	78	V923	I954	I901	V845
β7-strand (C-lobe)	CS4	76	I921	I952	I899	V843
D-helix (C-lobe)	CS3	53	I857	I888	I834	L798
F-helix (C-lobe)	CS2	None	None	None	None	L907
F-helix (C-lobe)	CS1	None	None	None	None	T903

[a] klifs.net.

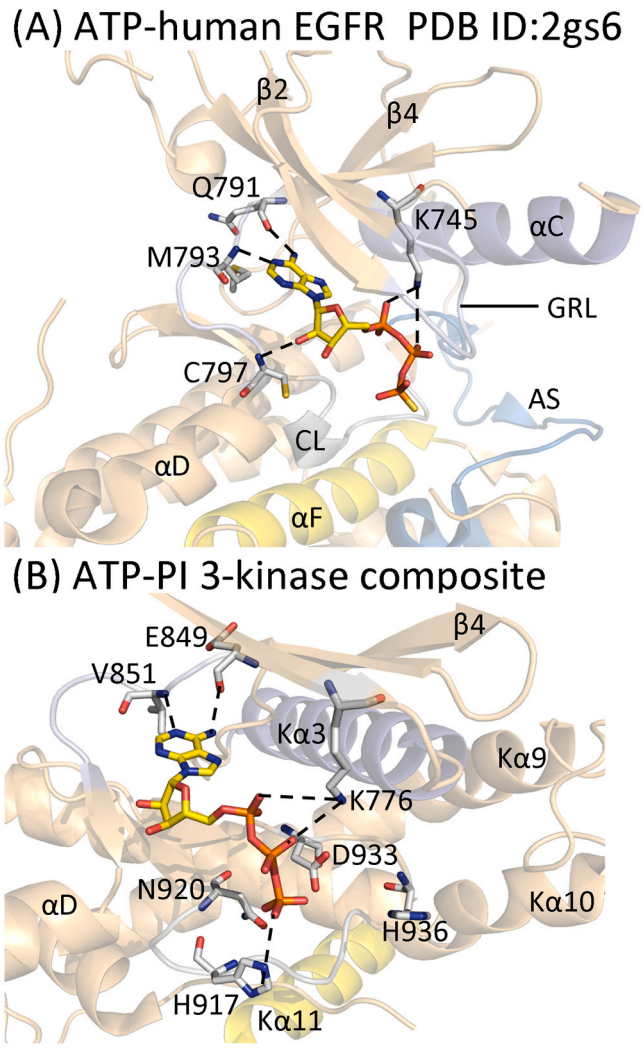

Fig. 4. ATP-binding sites. (A) human EGFR. (B) Superposition of human PI3Kα (PDB ID: 5dxh) and porcine PI3Kγ (PDB ID: 18ex). AS, activation segment; CL, catalytic loop; GRL, glycine-rich loop. The dashed lines depict polar bonds.

not to the β3-strand. In comparison, many low molecular weight ATP-competitive inhibitors of protein kinases and PI 3-kinases extend to the β3-strand and several course even further toward the αC-helix or Kα3-helix into the back pocket.

The PI 3-kinase pathway is activated in a broad range of cancers including leukemias and lymphomas [1–3,20,21]. Transformed cells must modify their metabolism and signaling to support cell growth and division to meet the needs of the hyperproliferative state. The PI 3-kinase pathway is a key signaling module that promotes nutrient uptake, macromolecule synthesis, and cell survival and is a very common target of activating oncogenic mutations. These alterations often involve direct mutational activation or amplification of genes encoding key components of the pathway; frequent findings include activation of *PIK3CA* and *AKT1* or loss of *PTEN*. Activating mutations at numerous sites in *PIK3CA* have been reported in tumors; however, three hot-spot mutations (H1047R, E542K, and E545K) account for about 80% of all somatic driver mutations in this gene [60]. These mutations alter different PI 3-kinase domains to enhance activity. For example, the H1047R mutation promotes the interaction of the p110 kinase domain with cell membranes and the E542K and E545K mutations disrupt the inhibitory interface of regulatory p85 [51].

H1047 occurs in the important Kα11-helix that interacts with the plasma membrane [51]. In the wild-type inactive enzyme, H1047 points inward toward the kinase domain. In contrast, the longer arginine chain in the mutant cannot be directed inward owing to steric hindrance and is directed outward where its positive charge is poised for membrane interaction and enzyme activation. X-ray crystal structures of the mutant enzyme suggest that this mutation also promotes formation of an active conformation. The hotspot E542K and E545K mutations mimic the action of receptor protein-tyrosine kinases by releasing autoinhibition. This action promotes conformational changes that expose the active site of PI3Kα at the membrane. The regulation of the activity of the PI 3-kinases is intricate. Among the processes involved in the regulation of enzyme activity include changes in conformation of the enzyme from active to inactive states as well as attraction to the plasma membrane where the PIP2 substrate resides.

3. Protein kinase and lipid kinase inhibitor classification and binding pockets

We divided small molecule protein kinase inhibitors into seven broad categories: I, I½, II, III, IV, V, and VI (Table 4) [56]. The majority of PI 3-kinase and ePK inhibitors bind in the ATP-binding site and are steady-state competitive inhibitors with respect to ATP. Type II protein kinase inhibitors bind to an inactive enzyme where the DF residues of the DFG string have the opposite orientation when compared with active protein kinases. The active structure is named DFG-D_{in} because the aspartate is directed inward toward the active site while type II inhibitors are referred to as the DFG-D_{out} configuration because the aspartate is directed away from the active site (See Refs. [49] for further descriptions and structures). Inhibitors bound to an inactive PI 3-kinase with DFG-D_{in} have been described and these correspond to type I½ inhibitors. Thus far, the DFG-D_{out} configuration has not been observed in PI 3-kinase structures and type II inhibitors are unlikely to be found. See Ref. [48] for a summary of type III and type IV aPK and ePK inhibitors. Type III ePK inhibitors are known, but not PI 3-kinase inhibitors. Type V ePK inhibitors are uncommon. Six targeted covalent ePK inhibitors (TCIs) that are FDA-approved are known (www.brimr.org/PKI/PKIs.htm) and wortmannin and other covalent PI 3-kinase antagonists, which are classified as type VI inhibitors, have been described [61,62].

Liao [63], van Linden et al. [64], and Kanev et al. [65] divided the region between the amino-terminal and carboxyterminal lobes of typical and atypical protein kinases including PI 3-kinases into the front pocket (front cleft), the gate area, and the back cleft. A general overview depicting these locations and their various sub-pockets is provided in Fig. 5 and Table 5. The gate area and back cleft make up HPII (hydrophobic pocket II) or the back pocket. Type I inhibitors typically bind within the front cleft or ATP-binding region. The gate area occurs between the front and back pockets. The back cleft occurs between the gatekeeper, the αC-(ePKs) or Kα3-helices (PI 3-kinases) and the DFG motif. Many type I½ inhibitors occupy both the front cleft and the initial part of the back cleft.

The average ePK drug-binding site is wider (from the αD- to αC-helix) than that of aPKs [48]. In contrast, the average aPK drug-binding site is deeper (from the DRH motif to the hinge) than that of ePKs. One of the goals in the development of small molecule protein kinase and lipid kinase inhibitors is to establish selectivity in order to reduce off-target side effects, a process that is enabled by evaluating the interaction of drugs with their target enzymes [66–68]. Owing to the differences in the sequences of the PI 3-kinase P-loop and the functionally similar ePK glycine-rich loop, such variances can be exploited in the development of inhibitors specific to either class of enzyme. Fabricating drug scaffold substituents that bind to residues lining the sub-pockets within the cleft plays a strategic role in drug discovery and development with the goal of maximizing drug affinity.

van Linden et al. [64] and Kanev et al. [65] formulated a

Table 4
Classification of small molecule protein kinase and PI 3-kinase inhibitors.[a]

Inhibitor type	Inhibitor properties
I	Binds in and around the adenine-binding pocket of an active enzyme
I½ A/B	Binds in and around the adenine-binding pocket of an inactive DFG-D_{in} enzyme
I½ A	Extends into the back cleft
I½ B	Does not extend into the back cleft
II A/B	Binds in and around the adenine-binding pocket of an inactive eukaryotic protein kinase DFG-D_{out} enzyme
III	Allosteric inhibitor bound near the adenine-binding pocket
IV	Allosteric inhibitor bound far from the adenine-binding pocket
V	Bivalent inhibitor spanning two kinase domain regions
VI	Covalent inhibitor

[a] Adapted from Ref. [56].

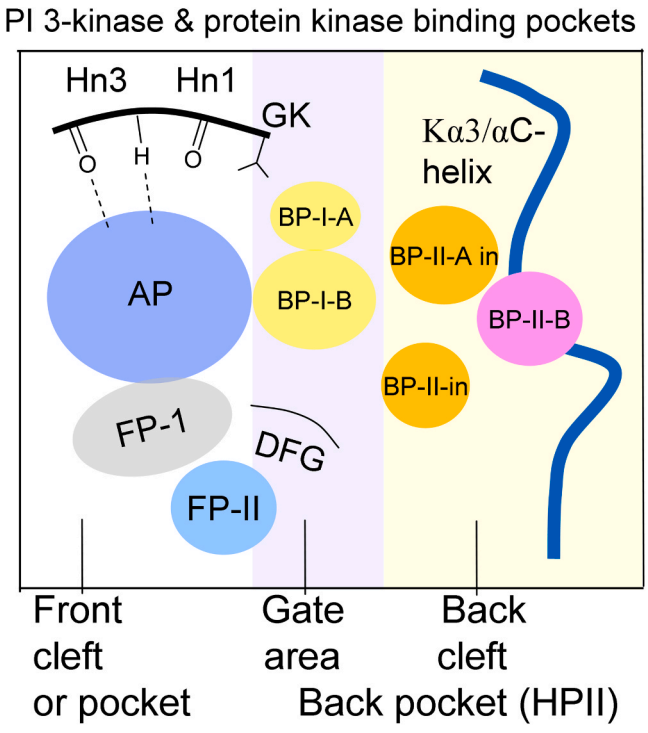

Fig. 5. Location of binding pockets for PI 3-kinases and protein kinases. AP, adenine pocket; GK, gatekeeper; Hn, hinge.

Table 5
Location of selected PI 3-kinase and protein kinase cleft and gate area residues.

Description[a]	Location	KLIFS residue no.[b]
P-loop (PI3K) or glycine-rich loop (ePK)	Front cleft	4–9
β2-strand CS7	Front cleft	11
β3-strand CS8	Front cleft	15
DRH (PI3K) or HRD (ePK)	Front cleft	70–72 or 68–70
Catalytic loop N	Front cleft	75
β7-strand CS6	Front cleft	77
β3-strand K	Gate area	17
αC-β4 penultimate back loop residue	Gate area	36
Gatekeeper residue	Gate area	45
The x of xDFG	Gate area	80
DFG	Gate area	81–83
Kα3-helix-D (PI3K) or αC-helix-E (ePK)	Back cleft	24
β4-strand RS4	Back cleft	38

[a] ePK, eukaryotic protein kinase.
[b] Refs. [64,65].

comprehensive directory that describes ligand and drug binding to more than 5500 human and mouse protein kinase domains. Their KLIFS (kinase–ligand interaction fingerprint and structure) compendium includes a list of 85 ligand binding-site residues occurring in both the amino-terminal and carboxyterminal lobes; this directory facilitates the classification of ligands and drugs depending upon their binding properties. These data assist in the detection and discovery of common and unique drug-enzyme interactions. Moreover, these authors devised a standard amino acid residue-numbering system that facilitates the comparison of different protein and lipid kinase targets. Table 3 describes the relationship of the KLIFS database nomenclature and the catalytic spine, shell, and regulatory spine amino acid residue-numbering system and Fig. 6 illustrates the location of the KLIFS residues within the kinase domain. Furthermore, these investigators launched a helpful free and searchable web site that is periodically updated that gives complete data on the interaction of protein and lipid kinases with ligands and drugs (klifs.net). Moreover, Carles et al. developed a comprehensive compendium of protein and lipid kinase inhibitors that are in clinical trials or have been approved [69]. They produced a searchable and non-commercial web site that is updated regularly and gives the structure of the various inhibitors, their protein targets, the therapeutic indications, the physicochemical drug properties, the year of first approval (if applicable), and the trade name (http://www.icoa.fr/pkidb/).

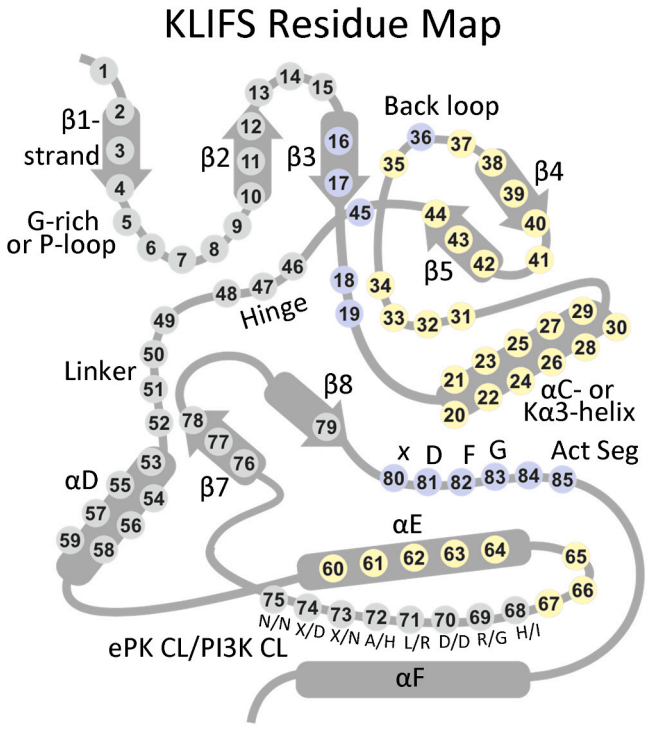

Fig. 6. The location of KLIFS residues within generic PI 3-kinase and protein kinase domains. Act Seg, activation segment. The ePK catalytic loop (CL) residues are given before the slash and the PI 3-kinase catalytic loop (CL) residues are given after the slash. Gray panels, Front cleft; Blue panels, Gate area; Yellow panels, Back cleft.

4. Breast cancer, chronic lymphocytic leukemia (CLL), small lymphocytic lymphoma (SLL), follicular lymphoma (FL), and marginal zone lymphoma (MZL)

Breast carcinoma is the leading cause of death from malignancies predominantly confined to women in both the United States and worldwide [70,71]. The number of estimated deaths per year in the United States in 2021 is about 44,000 and the number worldwide in 2020 is about 685,000 [70,71]. For purposes of treatment, breast cancers are grouped into three categories, which are not mutually exclusive: these include (i) overexpression of *ERBB2/HER2/NEU* or HER2-positive, (ii) hormone receptor-positive, and (iii) triple-negative breast cancer. Triple-negative breast cancer refers to those (i) without *ERBB2* amplification or overexpression and lacking (ii) estrogen and (iii) progesterone receptors. Wittliff reported that about 70% of breast cancers are estrogen receptor-positive [72] and Razavi et al. [73] reported that about 40% of estrogen receptor-positive, HER2-negative breast cancer patients bear *PIK3CA* mutations so that the number of potential candidates for treatment with alpelisib, which is described later, is large. Surgery is the principal treatment modality for localized breast cancer, followed by radiotherapy, chemotherapy, and adjuvant hormonal therapy (with tamoxifen or an aromatase inhibitor) for hormone receptor-positive tumors [7]. Many patients that are hormone receptor-positive benefit from treatment with anastrozole or letrozole. These are aromatase inhibitors that block the biosynthesis of the aromatic A ring of estradiol from androgenic precursors.

Chronic lymphocytic leukemia (CLL), which is a clonal B-cell disorder, is the most common form of leukemia in the Western hemisphere; it accounts for about 40% of all adult leukemias [70]. The estimated number of new cases in the United States in 2021 was 21,000 with a male to female ratio of 3:2 and the estimated number of deaths was 4000. The median age of patients at the time of diagnosis is about 70 years [74,75]. Its diagnosis is often incidental and based upon routine blood counts. Patients may present with fever, weight loss, night sweats, autoimmune hemolytic anemia, or immune thrombocytopenia. Physical examination may reveal axillary, cervical, and inguinal lymphadenopathy along with hepatomegaly and splenomegaly. A small percentage of chronic lymphocytic leukemia patients progress into an aggressive large cell lymphoma (LCL) by a transformation that is called the Richter syndrome. Laboratory studies indicate that chronic lymphocytic leukemia and large cell lymphoma cells share identical clonal origins. As a reference, the incidence of chronic myeloid leukemia has an incidence of about 9000 new cases in the United States per year [70] and these patients are treated with imatinib (Gleevec) and second- and third-generation Bcr-Abl non-receptor protein-tyrosine kinase inhibitors. These drugs are commercially profitable and suggest a baseline number of affected individuals that is required for the economic success of targeted small molecule therapeutic medicinals [56].

CLL patients have elevated lymphocyte counts with more than 5000 non-proliferating clonal mature B-cells/μL, a finding that persists for more than three months [74]. Histologically, these cells have scant cytoplasm and dense chromatin and they lack nucleoli. Such cells express B-cell markers including CD5, CD19, CD23 antigens and they weakly express CD20 and surface membrane immunoglobulin. Recombination of variable (V), diversity (D), and joining (J) genes takes place in the pre-germinal phase of B-cell development. Somatic mutations

occur in the VDJ rearrangement in normal B-cells. Approximately half of chronic lymphocytic leukemia patients have somatic mutations in the IgV gene (*IGHV-M*) and thus arise from post-germinal B-cells while a subset of patients has unmutated IgV (*IGHV-UM*) that arises from naïve B-cells. Patients lacking this mutation generally have a less favorable outcome.

Unlike most leukemias, the diagnosis of CLL is not necessarily an indication to begin treatment. Patients at early stages of the disease can be followed without specific therapy with a median survival greater than 10 years [76]. Patients who present with bone marrow failure would ordinarily have a median survival of only 1.5 years and thus require immediate therapy. The following agents have been approved by the FDA for the treatment of chronic lymphocytic leukemia: chlorambucil (1957), cyclophosphamide (1959), fludarabine (1991), alemtuzumab (2007), bendamustine (2008), ofatumumab (2009), rituximab in combination with fludarabine and cyclophosphamide (2010), obinutuzumab in combination with chlorambucil (2013), ibrutinib (2013), acalabrutinib (2017), and venetoclax (2019) [39,76]. Chlorambucil, cyclophosphamide, and bendamustine are alkylating agents; fludarabine is an anti-metabolite; alemtuzumab, ofatumumab, rituximab, and obinutuzumab are monoclonal antibodies. Acalabrutinib and ibrutinib are orally effective small molecule Bruton tyrosine kinase antagonists and venetoclax is an orally effective Bcl-2 inhibitor. Duvelisib and idelalisib are two PI 3-kinase inhibitors that are FDA-approved for the third-line treatment of CLL as described later.

Small lymphocytic lymphomas (SLL) represent about 7% of non-Hodgkin lymphomas or about 5700 cases per year in the United States [39,70,74]. These tumors involve lymph nodes with the same B-cell immunophenotype found in chronic lymphocytic leukemia without leukocytosis. Patients with SLL often present with asymptomatic lymphadenopathy. Splenomegaly is a common physical finding and the bone marrow is often involved. Other symptoms include painless swelling in the axilla, groin, or neck, fatigue, fever, night sweats, loss of appetite, and weight loss. This lymphoma is treated with any of several monoclonal antibodies such as alemtuzumab, brentuximab vedotin, ibritumomab tiuxetan, binutuzumab, polatuzumab vedotin, ofatumumab, rituximab, and tafasitamab. Numerous orally effective targeted therapies can also be prescribed including acalabrutinib, ibrutinib, selinexor, tazemetostat, and zanubrutinib. Three intravenous medications are also employed including belinostat, bortezomib, and romidepsin. Seinexor is a nuclear export inhibitor, tazemetostat is an EZH2 inhibitor, zanubrutinib is a BTK blocker, belinostat and romidepsin are histone deacetylase inhibitors, and bortezomib is a proteosome antagonist.

Follicular lymphomas (FL) are the second most commonly occurring lymphoma in the United States; they account for about one-fifth of all non-Hodgkin lymphomas and represent an incidence of about 16,000 cases annually in the United States in 2021 [70,77]. Follicular lymphoma is a mature B-cell lineage neoplasm. The patient median age at the time of diagnosis is 58 years. FL patients most often present with asymptomatic lymphadenopathy. Fever, night sweats, and weight loss occurs in about 15% of people. Most affected individuals (80–90%) present with advanced-stage disease (stage III or IV). Patients with limited-stage disease (about 20%) receive (i) cyclophosphamide, vincristine, prednisone, and bleomycin combination therapy or (ii) radiation therapy; many of these individuals are cured by these interventions. People with advanced-stage disease receive rituximab with (i) cyclophosphamide, vincristine, and prednisone (CVP), (ii) cyclophosphamide, doxorubicin, vincristine, and prednisone (CHOP), (iii) bendamustine, or (iv) fludarabine, mitoxantrone, and dexamethasone. Vincristine blocks cell division based upon its interaction with microtubules, mitoxantrone is a type II topoisomerase antagonist, and prednisone and dexamethasone are lympholytic glucocorticoids. Rituximab monotherapy is commonly used for maintenance. More recent therapies target the B-cell receptor pathway using BTK inhibitors such as ibrutinib and acalabrutinib [39,78]. FDA-approved inhibitors targeting PI 3-kinases are listed in Table 6 and four of them (copanlisib, duvelisib, idelalisib, and umbralisib) are prescribed for the treatment of follicular lymphoma.

Marginal zone lymphomas (MZL) make up about 8% of non-Hodgkin lymphomas, amounting to about 6500 new cases in the United States annually [70,79]. There are three subtypes of this disorder: nodal, splenic, and extra-nodal with mucosal associated lymphoid tissue involvement. The most common site of involvement of the mucosal subtype is in the stomach and this is usually associated with *Helicobacter pylori* infection. Early-stage MZL can be successfully treated with antibiotic therapy with complete regression in many cases with little recurrence. Treatment options include amoxicillin, clarithromycin, metronidazole, tetracycline or tinidazole. Patients with nodal disease present with peripheral or para-aortic lymphadenopathy and bone marrow involvement. Because nodal marginal zone lymphoma is most often an indolent disease, such patients are treated with active surveillance (i.e., watch and wait) until symptoms appear [80]. When treatment is necessary, options include radiation therapy, chemotherapy and immunotherapy with bendamustine and obinutuzumab. Ibrutinib is a targeted covalent inhibitor (TCI) of BTK that is approved for the treatment of MZL, CLL, SLL [39,78]. Patients with splenic involvement present with cytopenias, circulating malignant lymphocytes, and splenomegaly. About one-third of these patients do not require therapy. When treatment is deemed appropriate, several options exist. Some patients may receive a splenectomy; patients ineligible for surgery may receive low-dose radiation of the spleen. Other patients may be given rituximab, a monoclonal antibody, with or without chemotherapy. As noted in the next section, umbralisib is approved for the second-line treatment of patients with MZL.

5. Drug-PI 3-kinase interactions

Alpelisib is an orally effective thiazopyrrolidine derivative (Fig. 7A) [81] that is US FDA approved for the treatment of patients with advanced hormone receptor-positive, HER2-negative, *PIK3CA*-mutated breast cancer in combination with fulvestrant (an estrogen-receptor antagonist given IV). Wittliff reported that 70% of breast cancers are hormone-receptor-positive [72] and the incidence of *PIK3CA* mutations in hormone receptor-positive breast cancers is approximately 40% [73], indicating that alpelisib therapy may be appropriate for a large number of people [72,82]. In patients with *PIK3CA* mutations, progression-free survival after 20 months (median) follow up was 11.0 months in the

Table 6
FDA-approved PI 3-kinase inhibitors.

Drug (Code) Trade name	Year approved	Primary targets	Therapeutic indications[a]
Alpelisib (BLY719) Piqray	2019	PI3Kα	HR-positive, HER2-negative, *PIK3CA*-mutated advanced breast cancer, in combination with fulvestrant.
Copanlisib (BAY 80-6946) Aliquopa	2017	PI3Kα/δ	Third-line treatment of relapsed follicular lymphoma (FL).
Duvelisib (IPI-145) Copiktra	2018	PI3Kδ	Third-line treatment of relapsed or refractory (i) CLL, (ii) SLL, or (iii) FL.
Idelalisib (CAL-101) Zydelig	2014	PI3Kδ	Third-line treatment of relapsed or refractory (i) CLL in combination with rituximab, (ii) SLL, or (iii) FL.
Umbralisib (TGR-1202) Ukoniq	2021	PI3Kδ	Second-line treatment and third-line treatment of relapsed or refractory (i) MZL or (ii) FL, respectively.

[a] CLL, chronic lymphocytic leukemia; FL, follicular lymphoma; HER2, human epidermal growth factor receptor-2; HR, hormone receptor; MZL, marginal zone lymphoma; SLL, small lymphocytic lymphoma.

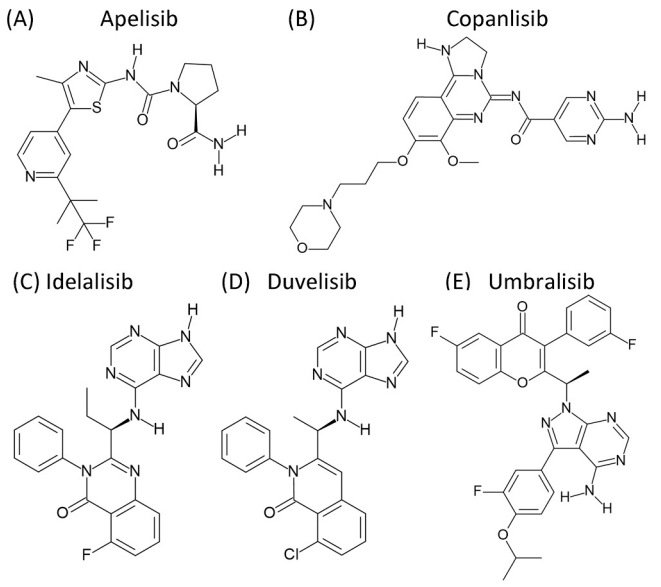

Fig. 7. Structures of the FDA-approved PI 3-kinase inhibitors.

combination alpelisib plus fulvestrant cohort and 5.7 months in the fulvestrant and placebo cohort [83]. In patients without a *PIK3CA* mutation, progression-free survival was 7.4 months in the combination alpelisib plus fulvestrant cohort and 5.6 months in the fulvestrant cohort. The overall complete response rate in patients with *PIK3CA*--mutated cancer was 26.6%; this response in those without mutations was 12.8%. The rationale for the FDA approval for patients bearing *PIKCA* mutations is explained by these results. The most common adverse events included hyperglycemia (52%), nausea (51%), decreased appetite (42%), diarrhea (40%), vomiting (31%), and maculopapular rash (13%) [84].

Alpelisib has greater affinity for PI3Kα (IC_{50} value of 4.6 nM) when compared with PI3Kβ (1160 nM), PI3Kδ (290 nM), and PI3Kγ (250 nM) [83]. The drug is a steady-state ATP-competitive inhibitor. That alpelisib is a PI3Kα inhibitor explains the observed hyperglycemia in patients treated with this drug [85]. The X-ray crystal structure of the drug bound to PI3Kα shows that the pyrrolidine nitrogen forms a hydrogen bond with the V851 N–H group and the drug amide group forms a hydrogen bond with the V851 carbonyl group of the third hinge residue (Fig. 8A). The alpelisib terminal N–H group forms a hydrogen bond with the carbonyl oxygen of S854, the fourth residue of the hinge-linker. The N–H and carbonyl group of the drug terminal carboxamide each form a hydrogen bond with Q859 within the αD-helix. This glutamine residue is not conserved among the PI 3-kinases and helps to explain in part the specificity of alpelisib.

The alpelisib-enzyme complex displays a face-to-edge aromatic interaction with Y836 and the drug interacts hydrophobically with I800, both components of the affinity pocket. Alpelisib makes hydrophobic contact with three spine residues (RS4, CS6/8) and the gatekeeper residue (Sh2). The medicinal also makes hydrophobic contact with the first residue of the P-loop (M772) and W780 of the β2-strand, which make up the specificity pocket. Apelisib makes hydrophobic contact with P778 of the β2-strand, K802 of the β3-strand, ^{849}EVVR^{852}, S854, and H855 of the hinge-linker, Q859 of the αD-helix, I932 (the x of xDFG), and DFG-D933. The drug occupies the front pocket and FP-II. The activation segment has the distinct U configuration near its terminus that is characteristic of an inactive DFG-D_{in} enzyme form. The distance from the α-carbon atom of DFG-D933 to that of PFxLT-F954 is 13.2Å, which is also indicative of a dormant enzyme form. Accordingly, alpelisib is classified as a type I½ inhibitor [56].

Copanlisib is an imidazoquinazoline derivative (Fig. 7B) [86] that is FDA approved for the third-line treatment of follicular lymphomas.

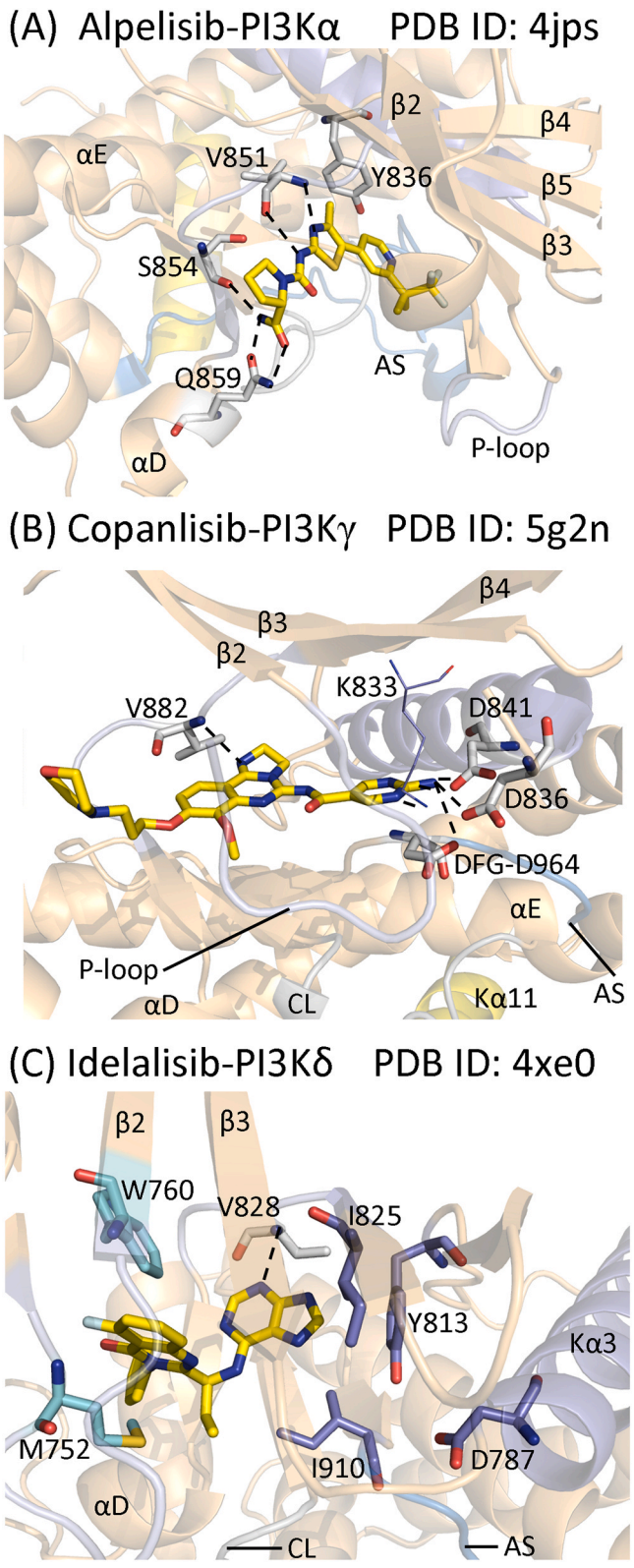

Fig. 8. (A) Alpelisib-PI3Kα. (B) Copanlisib-PI3Kγ. (C) Idelalisib-mouse PI3Kδ; the two residues with cyan carbon atoms are those of the specificity pocket (M752 is KLIFS residue-4; W760, KLIFS-12) and the four residues with dark blue carbon atoms are those of the affinity pocket (D787, KLIFS-24; Y813, KLIFS-38; I825, KLIFS-45; I910, KLIFS-80). The drug carbon atoms are yellow and the dashed lines represent polar bonds. AS, activation segment; CL, catalytic loop.

Follicular lymphoma patients in clinical trials exhibited an overall response rate of about 60%, a complete response of 14%, a median duration of response of 14.1 months, median progression-free survival of 12.5 months, and median overall survival of 42.6 months [87–89]. The most common adverse events reported were transient hyperglycemia in 50% of patients, transient hypertension in 29.6% of patients, diarrhea in 35.2% of patients, and neutropenia in 28.9% of patients. Copanlisib has a more favorable safety profile than the other agents in its class with no late-onset toxicities. However, unlike the other four PI 3-kinase inhibitors considered in this review, copanlisib is given intravenously on a weekly basis (days 1, 8, and 15 of each 28-day cycle).

Copanlisib is a potent ATP-competitive inhibitor of PI3Kα (IC_{50} value of 0.5 nM) and PI3Kδ (0.7 nM) while it is less effective against PI3Kβ (3.7 nM) and PI3Kγ (6.4 nM) [86]. The inhibition of PI3Kα explains the hyperglycemia observed in patients receiving this medicine [85]. The X-ray crystal structure shows that the imidazo nitrogen forms a hydrogen bond with the N–H group of V882 (the third hinge residue) and the terminal amino group of the drug forms hydrogen bonds with D836 in the β3-Kα3 loop, D841 of the Kα3-helix (a component of the affinity pocket), and DFG-D964 (Fig. 8B). The drug makes hydrophobic contact with two spine residues (CS8/RS4) and the gatekeeper (Sh2) residue. The agent also makes hydrophobic contact with the β1-strand K802, the β2-strand W812 (a part of the specificity pocket), the β3-strand I831 and K833, the Kα3-helix L838, and E880, I881, V882, and A885 of the hinge-linker segment, I963 (the x of xDFG), and DFG-D964. The drug occupies the front pocket, gate area, back pocket, and BP-I-A/B. The activation segment has a U configuration at its end and is characterized as an inactive enzyme form. The distance from the α-carbon atom of DFG-D964 to that of PFxLT-F985 is 15.0 Å, which is also indicative of a dormant enzyme form. Accordingly, copanlisib is classified as a type I½ inhibitor [56].

Idelalisib is an orally effective purine-quinazoline derivative (Fig. 7C) that is FDA-approved for the third-line treatment of follicular lymphoma and small lymphocytic lymphoma and as a combination therapy with rituximab (a chimeric monoclonal antibody directed against CD20 found on the surface of immune system B-cells) in the treatment of chronic lymphocytic leukemia. Herman et al. demonstrated that idelalisib promoted apoptosis in primary chronic lymphocytic leukemia cells ex vivo in a dose- and time-dependent manner. In contrast to malignant cells, idelalisib did not promote apoptosis in normal T cells or natural killer cells, nor did it diminish antibody-dependent cellular cytotoxicity [90]. Collectively, these studies provided the rationale for its clinical development as a first-in-class targeted therapy for chronic lymphocytic leukemia and related B-cell lymphoproliferative disorders [90].

The overall response rate in an early clinical trial of idelalisib was 57% in patients with follicular lymphomas, chronic lymphocytic leukemias, and small lymphocytic lymphomas [91]. The median progression-free survival and overall survival were estimated at 11.0 months and 20.3 months, respectively. The most common adverse events were fatigue, diarrhea, nausea, rash, chills, and pyrexia, whereas the most frequent grade 3 or above adverse events were diarrhea and pneumonitis. Grade 3 or higher elevation of serum transaminases occurred in 25% of patients. Idelalisib carries a black box warning for hepatotoxicity, severe diarrhea/colitis, pneumonitis, infection, and intestinal perforation [29] and early recognition of and intervention for these toxicities will mitigate risks and maintain meaningful disease control without compromising quality of life. In patients with long-standing relapsed chronic lymphocytic leukemia, the rate of progression-free survival in the idelalisib plus rituximab cohort was 93% versus 46% in the rituximab plus placebo cohort at 24 weeks. The most common adverse events in the combination group was pyrexia, fatigue, nausea, and diarrhea. Patients with follicular lymphoma or small lymphocytic lymphoma that received idelalisib monotherapy exhibited a rapid response to therapy (median time of 1.9 months) with a median 12.5 month response duration. The most common side effects were diarrhea, fatigue, nausea, cough, and pyrexia.

Idelalisib is a potent ATP-competitive inhibitor of PI3Kδ (IC_{50} value of 2.5 nM) while it is much less effective against PI3Kα (820 nM), PI3Kβ (565 nM), or PI3Kγ (89 nM) [92,93]. The X-ray crystal structure of idelalisib bound to murine PI3Kδ shows that *N*1 of purine forms a hydrogen bond with V828 of PI3Kδ, the third hinge residue (Fig. 8C). The drug makes hydrophobic contact with four spine residues (RS4, CS6/7/8) and one shell residue (Sh2, the gatekeeper). It also makes hydrophobic contact with the β1-strand T750 and F751, β2-strand P758 and L759, β3-strand I777, as well as V827, V828, D832, and T833 of the hinge-linker segment, and I910 (x of xDFG). Idelalisib also makes hydrophobic contact with P-loop M752 and β2-strand W760 of the specificity pocket, which are colored cyan. The four residues that make up the affinity pocket have blue carbon atoms and the drug makes hydrophobic contact with three of them (Y813, I825, I910). All of these residues are conserved in the human enzyme so that it is highly probable that idelalisib binds to the human protein in an identical fashion. The drug is found only in the front pocket of an active enzyme form (no U-shaped activation segment terminus and a DFG-D911 – PFxLT-F932 distance of 18.3 Å) and is classified as a type I inhibitor [56].

The three drugs form hydrogen bonds with the third hinge residue and make hydrophobic contact with RS4, the gatekeeper residue (Sh2), and catalytic spine residues CS8. Using the common KLIFS nomenclature, the specificity pocket of PI 3-kinases consists of KLIFS-4 (within the P-loop) and KLIFS-12 (β2-strand) and the affinity pocket is made up of KLIFS-24 (Kα3-helix), KLIFS-38 (β4-strand), KLIFS-45 (gatekeeper), and KLIFS-80 (x of xDFG) [52]. All three drugs interact hydrophobically with KLIFS-12 of the specificity pocket and KLIFS-38/45/80 of the affinity pocket. Alpelisib and idelalisib interact with KLIFS-4 of the specificity pocket and copanlisib forms a hydrogen bond with KLIFS-24 of the affinity pocket. Copanlisib fails to interact with KLIFS-4 of the specificity pocket and none of the three drugs interact hydrophobically with KLIFS-24 of the affinity pocket.

Duvelisib is an orally effective isoquinoline derivative (Fig. 7D) that is FDA-approved for the third-line treatment of relapsed or refractory chronic lymphocytic leukemia and small lymphocytic lymphoma and follicular lymphoma [93]. The drug is a potent ATP-competitive inhibitor of PI3Kδ with an IC_{50} value of 2.5 nM while it is less effective against PI3Kα (1600 nM), PI3Kβ (85 nM), or PI3Kγ (27 nM) [94]. Unfortunately, we lack X-ray crystal structures of this compound bound to its target. However, the structure of duvelisib is similar to that of idelalisib; duvelisib lacks a methyl group and one ring nitrogen and contains chlorine in place of fluorine at a comparable location (Fig. 7). Based upon the close structural similarities, it is likely that both drugs bind to their targets in a similar fashion and duvelisib is most likely a type I inhibitor that is found only within the front pocket.

In preclinical studies, duvelisib produced rapid inhibition of AKT phosphorylation (a downstream marker of PI 3-kinase signaling) [38,95] and reduced serum levels of various chemokines and cytokines including CXCL9, CXCL10, CXCL11, and interleukin-10. Duvelisib induced apoptosis in CLL lymphocytes, with minimal cytotoxicity against normal B-cells [96,97]. On the other hand, the drug was somewhat cytotoxic to normal T cells and natural killer cells. Duvelisib also resulted in approximately twice the cell death when compared with the PI3Kδ inhibitor idelalisib or the PI3Kα/δ antagonist copanlisib. In a pivotal phase 3 clinical trial (DUO study), duvelisib monotherapy resulted in a statistically significant improvement in progression-free survival and the overall response rate compared with ofatumumab in patients with relapsed or refractory chronic lymphocytic leukemia/small lymphocytic lymphoma including those with 17p deletions and p53 mutations [98]. Clinically meaningful reductions in target lymph nodes were observed in most patients treated with duvelisib (85%), representing a statistically significant treatment effect over ofatumumab (16%) ($P < .0001$).

Umbralisib is an orally effective pyrazolo[3,4-*d*]pyrimidine derivative that inhibits PI3Kδ and is FDA-approved for the second-line

treatment of marginal zone lymphoma and third-line treatment of follicular lymphoma. This drug is a specific inhibitor of PI3Kδ with an IC_{50} value of 22 nM while its inhibitory potency against PI3Kα/β/γ is greater than 1000 nM [99]. Preclinical studies showed that umbralisib decreased mTOR activity and inhibited the phosphorylation of the eukaryotic translation initiation factor 4E (eIF4E)-binding protein 1 (4E-BP1) that lead to the suppression of Myc translation to silence Myc-dependent transcription [100]. The overall response in an early clinical trial in patients with relapsed or refractory chronic lymphocytic leukemia, small lymphocytic lymphoma, and B-cell and T-cell non-Hodgkin lymphoma was 37%. The partial response rate was 33% [101]. The most common adverse events were diarrhea (43%), nausea (42%), and fatigue (31%). The most common grade 3 or 4 adverse events were neutropenia (13%), anemia (9%), and thrombocytopenia (7%). In a clinical study of relapsed or refractory marginal zone lymphoma, the overall response rate was 55% with a complete response in 10% of patients [102]. The 12-month progression-free survival was 71%. Clinical trials such as these led to the FDA approval of umbralisib. This agent also inhibits casein kinase-1ε, a protein serine/threonine kinase. The role that blockade of this enzyme in the therapeutic response to umbralisib is unknown. Unfortunately, we lack X-ray crystal structures of this compound bound to its targets. The IC_{50} values for the five FDA-approved PI 3-kinase inhibitors considered in this review are listed in Table 7.

6. Analyses of the physicochemical properties of the FDA-approved PI 3-kinase inhibitors

6.1. Lipinski's rule of five (Ro5)

Alpelisib, idelalisib, duvelisib, and umbralisib are orally bioavailable, but copanlisib must be given intravenously. Pharmacologists and medicinal chemists have searched for advantageous drug-like chemical properties that yield drugs that are orally effective. Lipinski's "rule of five" is a computational and experimental approach that is used to estimate solubility, membrane permeability, and oral bioavailability in the drug-development setting [103–110]. It is a rule of thumb that assesses drug-likeness and governs whether an agent has the chemical and physical properties that suggest it would be orally effective. The Lipinski criteria were based upon data indicating that most orally effective medicinals are small, moderately lipophilic, molecules. The Ro5 criteria are used during drug development as pharmacologically effective lead compounds are successively optimized to increase their potency while maintaining their physicochemical properties and selectivity.

The Ro5 implies that a drug is more likely to be orally effective when (i) the calculated Log P (cLogP) is 5 or less, when (ii) there are 5 or fewer hydrogen-bond donors, when (iii) there are 10 (5×2) or fewer hydrogen-bond acceptors, and when (iv) the molecular weight is 500 (5×100) or less [103]. The partition coefficient (P) is the ratio of the solubility of the un-ionized drug in the organic phase of water-saturated n-octanol divided by its solubility in the aqueous phase. The P value is a surrogate for the hydrophobicity of a compound; the greater the P value, the greater the hydrophobicity. The number of hydrogen-bond donors is the sum of NH and OH groups in the compound. The number of hydrogen-bond acceptors is the number of heteroatoms lacking a formal positive charge except for heteroaromatic oxygen and sulfur atoms, heteroaromatic pyrrole nitrogen atoms, halogen atoms, and higher oxidation states of nitrogen, phosphorus and sulfur, but it includes the oxygen atoms bonded to them.

The Ro5 is based on the physicochemical properties of more than two thousand reference pharmaceuticals [103]. The five FDA-approved PI 3-kinase inhibitors have a calculated Log of the partition coefficient of less than five, fewer than five hydrogen bond donors, and fewer than 10 hydrogen bond acceptors. Of the five drugs, four have molecular weights less than 500 except umbralisib and they fall within Lipinski's Ro5 (Table 8). It appears that the oral ineffectiveness of copanlisib represents an anomaly.

Table 7
Drug IC_{50} values (nM) for various human PI 3-kinase isoforms.

Drug	110α	110β	110δ	110γ	Ref.
Alpelisib	4.6	1160	290	250	[83]
Copanlisib	0.5	3.7	0.7	6.4	[86]
Duvelisib	1600	85	2.5	27	[94]
Idelalisib	820	565	2.5	89	[92]
Umbralisib	> 10,000	1120	22	1060	[99]

6.2. The importance of lipophilicity and ligand efficiency

6.2.1. Lipophilic efficiency, LipE

After the formulation of Lipinski's Ro5 in 2001 [103], subsequent analyses of the physicochemical properties of orally effective medicines led to several refinements [104–110]. Lipophilic efficiency (LipE), for example, is a property that combines potency and lipophilic-driven binding as a strategy to increase binding efficacy during drug development. The following formulas are used to calculate lipophilic efficiency:

$$\text{LipE} = \text{pIC}_{50} - \text{cLogD} \text{ or } \text{LipE} = \text{p}K_\text{i} - \text{cLogD}$$

Like its usage to express the molar hydrogen ion concentration as pH, the operator p in this equation denotes the negative of the Log of the IC_{50} or K_i. Additionally, cLogD is the calculated Log of the Distribution coefficient; this quantity represents the ratio of the amount of the ionized and un-ionized drug in the organic phase divided by its solubility in the aqueous phase of immiscible n-octanol/water at a specified pH, which is usually near 7.

The second term of the equation (−cLogD or minus cLogD) reflects the lipophilicity of a pharmaceutical where c indicates that the value is calculated based upon an algorithm representing the properties of thousands of reference compounds. The greater the solubility of a compound in the organic phase of an immiscible n-octanol/water mixture, the greater its lipophilicity. Leeson and Springthorpe suggested that drug lipophilicity, as assessed by its −cLogP value, is one of the more important properties that should be evaluated during drug development [106]. Their use of −cLogP was based upon studies performed before the use of the distribution coefficient (D) became in common use. For practical considerations, either cLogP or cLogD can be used to compare a series of lead compounds.

Compounds with higher lipophilicity may exhibit enhanced binding to adventitious targets and this property may lead to an increase in the type of adverse events observed in the therapeutic setting. One objective during drug development is to increase potency without simultaneously increasing lipophilicity. Monitoring lipophilic efficiency (LipE) aids in the optimization of lead compounds during drug development; moreover, the same assay should be used to make such comparisons valid [106,109]. To cite one prominent example, progress in the development of crizotinib from lead compounds as described by Cui et al. was monitored by using lipophilic efficiency as a numerical index of binding effectiveness [111]. Crizotinib is approved for the treatment of ALK-positive and ROS1-positive non-small cell lung cancer [112–114].

cLogD can be calculated by computer algorithms in a matter of minutes. Because the experimental determination of LogD is laborious, such measurements are performed in only limited situations. Increasing potency and decreasing the lipophilicity during drug development generally produces drugs with improved pharmacological properties. Smith reported that optimal values of lipophilic efficiency values range from 5 to 10 [105]. Except for umbralisib with a LipE value of 2.62, the other four FDA-approved PI 3-kinase inhibitors have values that are within or are very close to this range (Table 9).

6.2.2. Ligand efficiency, LE

The ligand efficiency (LE) is a property that relates potency, or

Table 8
Properties of FDA-approved small molecule PI 3-kinase inhibitors.[a]

Drug	PubChem CID	Formula	MW (Da)	HD[b]	HA[c]	cLogP[d]	Rotatable bonds	PSA[e] (Å^2)	Ring count	CA[f]	Complexity[g]
Alpelisib[h]	56649450	$C_{19}H_{22}F_3N_5O_2S$	441.5	2	8	2.31	4	129	3	1	663
Copanlisib	135565596	$C_{23}H_{28}N_8O_4$	480.5	2	9	1.13	7	140	5	0	974
Idelalisib[h]	11625818	$C_{22}H_{18}FN_7O$	415.4	2	7	2.80	5	99.2	5	1	685
Duvelisib[h]	50905713	$C_{22}H_{17}ClN_6O$	416.9	2	5	3.71	4	86.8	5	1	668
Umbralisib[h]	72950888	$C_{31}H_{24}F_3N_5O_3$	571.5	1	10	5.03	6	105	6	1	1020

[a] All data from NIH PubChem except for cLogP (which was computed using MedChem Designer™, version 2.0, Simulationsplus, Inc. Lancaster, CA 93534).
[b] No. of hydrogen bond donors.
[c] No. of hydrogen bond acceptors.
[d] Calculated Log of the partition coefficient.
[e] PSA, Polar surface area.
[f] CA, chiral atoms.
[g] Values obtained from https://pubchem.ncbi.nlm.nih.gov/.
[h] Orally bioavailable.

Table 9
Lipophilic efficiency (LipE) and ligand efficiency (LE) values and primary targets of FDA-approved PI 3-kinase inhibitors.

Drug	Target[a]	K_i (nM)[b]	pK_i	cLogP[c]	LipE[d]	N[e]	LE[f]
Alpelisib	PI3Kα	4.6	8.34	2.31	6.03	30	0.392
Copanlisib	PI3Kα/δ	0.5	9.30	1.13	8.17	35	0.374
Idelalisib	PI3Kδ	2.5	8.60	2.80	5.80	31	0.391
Duvelisib	PI3Kδ	2.5	8.60	3.71	4.89	30	0.404
Umbralisib	PI3Kδ	22.2	7.65	5.03	2.62	42	0.256

[a] PI3K, phosphatidylinositol 3-kinase.
[b] Representative values obtained from www.ebi.ac.ug/chembl/ and from klifs.net.
[c] Calculated value of the Log of the partition coefficient using MedChem Designer™ version 2.0 Simulationsplus, Inc. Lancaster CA 93534, USA.
[d] LipE = pIC$_{50}$ − cLogP, where cLogP is the calculated value of the Log of the partition coefficient.
[e] N, Number of heavy atoms.
[f] LE = −2.303 RT (LogK_{eq})/N where N is the number of heavy (non-hydrogen) atoms in the drug and T = 310 K.

binding affinity, to the number of non-hydrogen atoms (heavy atoms) of a drug. The following formula is used to calculate this property:

$$LE = \Delta G^{\circ\prime}/N = -RT\ \ln K_{eq}/N = -2.303RT\ \text{Log}\ K_{eq}/N$$

$\Delta G^{\circ\prime}$ is the standard free energy change of an agent binding to its enzyme target at neutral pH, R represents the universal gas constant or energy-temperature coefficient, (0.00198 kcal/° mol), T signifies the absolute temperature in degrees Kelvin, K_{eq} is the value of the equilibrium constant, and N represents the number of heavy atoms (non-hydrogen atoms) in the compound. Hopkins et al. suggested that optimal values of ligand efficiency are greater than 0.3 kcal/mol [108]. The IC$_{50}$ or K_i values are proxies for the equilibrium constant. At a physiological temperature of 37 °C (310 K), this equation becomes – (2.303 × (0.00198 kcal/mol K) × 310 K Log K_{eq})/N or – 1.41 Log K_{eq}/N. Ligand efficiency was initially suggested as a procedure for comparing drug affinities based upon the average binding energy per atom. Ligand efficiency is especially useful in fragment-based drug discovery protocols and, like lipophilic efficiency, its use aids in the selection of lead compound derivatives [109].

Ligand efficiency corresponds to the binding affinity per heavy atom of the ligand or agent of interest. The value of N is a substitute for the molecular weight. The equation that is used to calculate ligand efficiency indicates that the value is directly proportional to – Log K_{eq} (a positive number), or the binding affinity, and is inversely proportional to the sum of heavy atoms. The values of ligand efficiency for the FDA-approved small molecule PI 3-kinase inhibitors based upon representative IC$_{50}$ values are provided in Table 9. Four of the FDA-approved PI 3-kinase inhibitors have a ligand efficiency greater than 0.3 except umbralisib. The values for lipophilic efficiency (LipE) and ligand efficiency (LE) listed in Table 9 are based on data obtained under different experimental conditions. Accordingly, these values cannot be used to make a direct comparison of the drugs owing to the difference in assay conditions used to obtain the data. However, these data were obtained from different drug discovery projects and are intended to provide representative values.

6.3. Additional chemical descriptors of orally effective drugs

To enhance criteria associated with oral effectiveness, not-unexpectedly, the Ro5 has generated many corollaries. For example, Veber et al. reported that the polar surface area (PSA) and the number of rotatable bonds differentiates between agents that are and are not orally bioavailable for a large series of substances in rats [110]. These investigators found that compounds with polar surface areas less than or equal to 140 Å^2 are orally effective. The polar surface area represents the space over all polar atoms, primarily oxygen and nitrogen, but also including any linked hydrogen atoms. Furthermore, Veber et al. suggested that the optimal number of rotatable bonds should be 10 or less [110]. This property mirrors the molecular flexibility (degrees of freedom) and is postulated to control passive membrane permeation. The five FDA-approved PI 3-kinase antagonists fulfill Veber's two criteria. Moreover, Oprea found that the number of rings in most orally approved drugs is three or greater, the number of rigid bonds is 18 or greater, and the number of rotatable bonds is six or greater [115] and the five drugs we have considered fulfill the three Oprea criteria. Based upon these two analyses, the number of rotatable bonds in orally effective drugs should range between six and ten.

The molecular complexity of a drug is based upon its composition, structural features, and any symmetry elements. The parameter is calculated using the Bertz/Hendrickson/Ihlenfeldt algorithm [116,117]. It is based upon the identity and number of the component atoms, the nature of the chemical linkages, and their bonding pattern. The molecular complexity ranges from zero for simple ions to several thousand for complex natural products. Intuitively, larger chemicals generally possess a higher molecular complexity value than smaller ones. The molecular complexity values for the drugs considered in this review were obtained from PubChem (https://pubchem.ncbi.nlm.nih.gov/). Of the five FDA-approved PI 3-kinase inhibitors, the molecular complexity is greatest for umbralisib (Table 9). There are no optimal or recommended molecular complexity values for orally effective drugs; however, this property may be helpful in determining the ease or difficulty of drug synthesis, an important consideration in the commercial production of pharmaceutical agents.

7. PI 3-kinase inhibitor toxicities

The discovery of the phosphatidylinositol 3-kinase (PI 3-kinase) pathway constitutes a major advance in the understanding of

eukaryotic signal transduction. The high frequency of PI 3-kinase pathway mutations in many cancers has promoted a strategy of targeting these oncogenic mutants. Although there have been some promising results, targeting PI 3-kinase itself has proven challenging. The limited success is due in part to the multiple enzyme isoforms that are so closely related. The development of PI 3-kinase inhibitors as anticancer agents has been limited by modest monotherapeutic efficacy and significant adverse effects. Increasing our understanding of the complex regulatory feedback mechanisms that are activated in response to PI 3-kinase inhibition may suggest strategies to increase the efficacy of PI 3-kinase inhibitors and to minimize adverse effects and increase the usefulness of this class of drug treatment options for multiple cancer varieties. Given the pivotal role that PI 3-kinases play in a multitude of physiological functions, there is a substantial potential for the abrogation of essential cellular functions by PI 3-kinase inhibitors in normal tissues, so-called "on-target" drug toxicity [19]. It is, therefore, no surprise that progress in the clinical development of PI 3-kinase inhibitors as single-agent anti-cancer therapies has been reduced by the difficulty of developing agents with an optimal therapeutic window.

Loss of appetite is a serious problem in the clinical management of nearly all cancer patients [118] and this is a common finding in patients receiving PI 3-kinase antagonists. Some of the most common side effects resulting from the clinical use of PI 3-kinase inhibitors are nausea, vomiting, diarrhea, and colitis. While these are common side effects for many drugs, the mechanism for idelalisib-induced colitis is thought to be mediated by enhanced inflammation occurring in response to gut pathogens [119] and there is some evidence that points to this dose-limiting toxicity as a PI 3-kinase class effect because these enzymes play a significant role in gut immunity, motility, and neurotransmission [120]. Pneumonitis is a common side effect associated with the PI 3-kinase inhibitors [119,121]. There is an increased risk of infection due to the immunomodulatory effects of PI 3-kinase inhibitors that are likely mediated through the enhanced inflammation that results in response to pathogens present in the airways. Moreover, the PI 3-kinase pathway plays an important role in pulmonary smooth muscle development, contractility, and inflammation. Many studies have focused on the regulation of the PI 3-kinase pathway as a way to control asthma and chronic obstructive pulmonary disease [122].

The integument and skin function physiologically to promote thermoregulation and prevent dehydration while also providing protection against pathogens. A maculopapular rash is one of the common dose-limiting toxicities reported for PI 3-kinase inhibitors [19] including idelalisib [123]. The mechanism for idelalisib-induced rash is thought to be mediated at least in part through enhanced inflammation occurring in response to such pathogens. On the positive side, it has been suggested that clinicians could use the development of skin rashes as a pharmacodynamic biomarker for drug titration [124] in the same way that rashes are used to titrate the dose of EGFR inhibitors [125].

PI3Kα-specific inhibitors block insulin-stimulated glucose uptake in vivo [85] resulting in insulin resistance. This is supported by findings that PI3Kα is the dominant isoform required to mediate insulin and IGF-I signal transduction in muscle, adipocytes, and liver. These organs play a key role in the regulation of glucose metabolism. Insulin action in the liver is critical for maintaining normoglycemia as glucose storage (glycogenesis), breakdown (glycolysis) and production (glycogenolysis and gluconeogenesis) are all regulated by insulin [126]. The inhibition of insulin signaling promotes glycogen breakdown in the liver and prevents glucose uptake in the skeletal muscle and adipose tissue and results in transient hyperglycemia that occurs within a few hours of PI 3-kinase inhibition. The hyperglycemia is usually transient owing to the compensatory release of insulin from the pancreas that restores normal glucose homeostasis. However, the hyperglycemia may be prolonged or exacerbated in patients with any degree of insulin resistance and this may necessitate discontinuation of PI 3-kinase inhibitor therapy. Data suggest that insulin feedback induced by PI 3-kinase inhibitors reactivate the PI3K-mTOR signaling axis in tumors, thereby compromising their effectiveness [127].

The use of PI 3-kinase inhibitors such as copanlisib, idelalisib, duvelisib, and umbralisib has not been as successful in the treatment of B-cell malignancies as the use of small molecule BTK inhibitors in the treatment of these disorders in terms of efficacy and side effects. Because resistance to BTK antagonists invariably occurs, however, the use of third-line PI 3-kinase inhibitors represents an important follow-up option. Apelisib has been relatively effective in the treatment of breast cancers bearing *PIK3CA* mutations. Ideal drugs are those that inhibit the mutant protein and promote maximal cancer-specific benefits while avoiding general toxicities owing to a lack of blockade of non-mutant PI 3-kinases. The development of drugs that specifically target mutant enzymes is a long-term goal and time will tell whether it is achievable.

Conflict of interest

The author is unaware of any affiliations, memberships, or financial holdings that might be perceived as affecting the objectivity of this review.

Acknowledgment

I thank Dr. Albert J. Kooistra for providing the template depicted in Fig. 5. I thank Drs. Ruth Nussinov, Mingzhen Zhang, and Hyunbum Jang for sharing their insight on the nature of active and inactive PI 3-kinases. I thank Laura M. Roskoski for providing editorial and bibliographic assistance. I also acknowledge the assistance of Jasper Martinsek and Josie Rudnicki for their help in preparing the figures and W.S. Sheppard and Pasha Brezina for their help in structural analyses. The colored figures in this paper were evaluated to ensure that their perception was accurately conveyed to colorblind readers [128].

References

[1] L.M. Thorpe, H. Yuzugullu, J.J. Zhao, PI3K in cancer: divergent roles of isoforms, modes of activation and therapeutic targeting, Nat. Rev. Cancer 15 (2015) 7–24.
[2] F. Janku, T.A. Yap, F. Meric-Bernstam, Targeting the PI3K pathway in cancer: are we making headway? Nat. Rev. Clin. Oncol. 15 (2018) 273–291.
[3] M.N. Paddock, S.J. Field, L.C. Cantley, Treating cancer with phosphatidylinositol-3-kinase inhibitors: increasing efficacy and overcoming resistance, J. Lipid Res. 60 (2019) 747–752.
[4] R. Roskoski Jr., The ErbB/HER receptor protein-tyrosine kinases and cancer, Biochem. Biophys. Res. Commun. 319 (2004) 1–11.
[5] R. Roskoski Jr., The ErbB/HER family of protein-tyrosine kinases and cancer, Pharmacol. Res. 79 (2014) 34–74.
[6] R. Roskoski Jr., ErbB/HER protein-tyrosine kinases: structure and small molecule inhibitors, Pharmacol. Res. 87 (2014) 42–59.
[7] R. Roskoski Jr., Small molecule inhibitors targeting the EGFR/ErbB family of protein-tyrosine kinases in human cancers, Pharmacol. Res. 139 (2019) 395–411.
[8] R. Roskoski Jr., The role of fibroblast growth factor receptor (FGFR) protein-tyrosine kinase inhibitors in the treatment of cancers including those of the urinary bladder, Pharmacol. Res. 151 (2020), 104567.
[9] R. Roskoski Jr., The role of small molecule platelet-derived growth factor receptor (PDGFR) inhibitors in the treatment of neoplastic disorders, Pharmacol. Res. 129 (2018) 65–83.
[10] R. Roskoski Jr., Signaling by Kit protein-tyrosine kinase–the stem cell factor receptor, Biochem. Biophys. Res. Commun. 337 (2005) 1–13.
[11] R. Roskoski Jr., Structure and regulation of Kit protein-tyrosine kinase–the stem cell factor receptor, Biochem. Biophys. Res. Commun. 338 (2005) 1307–1315.
[12] R. Roskoski Jr., The role of small molecule Kit protein-tyrosine kinase inhibitors in the treatment of neoplastic disorders, Pharmacol. Res. 133 (2018) 35–52.
[13] R. Roskoski Jr, A. Sadeghi-Nejad, Role of RET protein-tyrosine kinase inhibitors in the treatment RET-driven thyroid and lung cancers, Pharmacol. Res. 128 (2018) 1–17.
[14] R. Roskoski Jr., ROS1 protein-tyrosine kinase inhibitors in the treatment of ROS1 fusion protein-driven non-small cell lung cancers, Pharmacol. Res. 121 (2017) 202–212.
[15] R. Roskoski Jr., Vascular endothelial growth factor (VEGF) signaling in tumor progression, Crit. Rev. Hematol. Oncol. 62 (2007) 179–213.
[16] R. Roskoski Jr., VEGF receptor protein-tyrosine kinases: structure and regulation, Biochem. Biophys. Res. Commun. 375 (2008) 287–291.
[17] R. Roskoski Jr., Vascular endothelial growth factor (VEGF) and VEGF receptor inhibitors in the treatment of renal cell carcinomas, Pharmacol. Res. 120 (2017) 116–132.

[18] T.F. Franke, D.R. Kaplan, L.C. Cantley, A. Toker, Direct regulation of the Akt proto-oncogene product by phosphatidylinositol-3,4-bisphosphate, Science 275 (1997) 665–668.
[19] C.M. Buchanan, K.L. Lee, P.R. Shepherd, For better or worse: the potential for dose limiting the on-target toxicity of PI 3-kinase inhibitors, Biomolecules 9 (2019) 402.
[20] G. Hoxhaj, B.D. Manning, The PI3K-AKT network at the interface of oncogenic signalling and cancer metabolism, Nat. Rev. Cancer 20 (2020) 74–88.
[21] T.J. Phillips, J.M. Michot, V. Ribrag, Can next-generation PI3K inhibitors unlock the full potential of the class in patients with B-cell lymphoma? Clin. Lymphoma Myeloma Leuk. 21 (2021) 8–20.
[22] L. Braccini, E. Ciraolo, C.C. Campa, A. Perino, D.L. Longo, G. Tibolla, M. Pregnolato, Y. Cao, B. Tassone, F. Damilano, M. Laffargue, E. Calautti, M. Falasca, G.D. Norata, J.M. Backer, E. Hirsch, PI3K-C2γ is a Rab5 effector selectively controlling endosomal Akt2 activation downstream of insulin signalling, Nat. Commun. 6 (2015) 7400.
[23] M. Whitman, C.P. Downes, M. Keeler, T. Keller, L. Cantley, Type I phosphatidylinositol kinase makes a novel inositol phospholipid, phosphatidylinositol-3-phosphate, Nature 332 (1988) 644–646.
[24] A. Wallroth, V. Haucke, Phosphoinositide conversion in endocytosis and the endolysosomal system, J. Biol. Chem. 293 (2018) 1526–1535.
[25] A. Visentin, F. Frezzato, F. Severin, S. Imbergamo, S. Pravato, L. Romano Gargarella, S. Manni, S. Pizzo, E. Ruggieri, M. Facco, A.M. Brunati, G. Semenzato, F. Piazza, L. Trentin, Lights and shade of next-generation PI3K inhibitors in chronic lymphocytic leukemia, OncoTargets Ther. 13 (2020) 9679–9688.
[26] S. Zhou, SH2 domains recognize specific phosphopeptide sequences, Cell 72 (1993) 767–778.
[27] L.C. Cantley, Z. Songyang, Specificity in recognition of phosphopeptides by src-homology 2 domains, J. Cell Sci. Suppl. 18 (1994) 121–126.
[28] M.D. Goncalves, B.D. Hopkins, L.C. Cantley, Phosphatidylinositol 3-kinase, growth disorders, and cancer, N. Engl. J. Med. 379 (2018) 2052–2062.
[29] A. Hanlon, D.M. Brander, Managing toxicities of phosphatidylinositol-3-kinase (PI3K) inhibitors, Hematol. Am. Soc. Hematol. Educ. Program 2020 (2020) 346–356.
[30] A. Wiestner, The role of B-cell receptor inhibitors in the treatment of patients with chronic lymphocytic leukemia, Haematologica 100 (2015) 1495–1507.
[31] A. Mócsai, J. Ruland, V.L. Tybulewicz, The SYK tyrosine kinase: a crucial player in diverse biological functions, Nat. Rev. Immunol. 10 (2010) 387–402.
[32] R.W. Hendriks, S. Yuvaraj, L.P. Kil, Targeting Bruton's tyrosine kinase in B cell malignancies, Nat. Rev. Cancer 14 (2014) 219–232.
[33] R. Roskoski Jr., RAF protein-serine/threonine kinases: structure and regulation, Biochem. Biophys. Res. Commun. 399 (2010) 313–317.
[34] R. Roskoski Jr., Targeting oncogenic Raf protein-serine/threonine kinases in human cancers, Pharmacol. Res. 135 (2018) 239–258.
[35] R. Roskoski Jr., MEK1/2 dual-specificity protein kinases: structure and regulation, Biochem. Biophys. Res. Commun. 417 (2012) 5–10.
[36] R. Roskoski Jr., Allosteric MEK1/2 inhibitors including cobimetinib and trametinib in the treatment of cutaneous melanomas, Pharmacol. Res. 117 (2017) 20–31.
[37] R. Roskoski Jr., ERK1/2 MAP kinases: structure, function, and regulation, Pharmacol. Res. 66 (2012) 105–143.
[38] R. Roskoski Jr., Targeting ERK1/2 protein-serine/threonine kinases in human cancers, Pharmacol. Res. 142 (2019) 151–168.
[39] R. Roskoski Jr., Ibrutinib inhibition of Bruton protein-tyrosine kinase (BTK) in the treatment of B cell neoplasms, Pharmacol. Res. 113 (2016) 395–408.
[40] F. Sanchez-Vega, M. Mina, J. Armenia, W.K. Chatila, A. Luna, K.C. La, S. Dimitriadoy, D.L. Liu, H.S. Kantheti, S. Saghafinia, D. Chakravarty, F. Daian, Q. Gao, M.H. Bailey, W.W. Liang, S.M. Foltz, I. Shmulevich, L. Ding, Z. Heins, A. Ochoa, B. Gross, J. Gao, H. Zhang, R. Kundra, C. Kandoth, I. Bahceci, L. Dervishi, U. Dogrusoz, W. Zhou, H. Shen, P.W. Laird, G.P. Way, C.S. Greene, H. Liang, Y. Xiao, C. Wang, A. Iavarone, A.H. Berger, T.G. Bivona, A.J. Lazar, G. D. Hammer, T. Giordano, L.N. Kwong, G. McArthur, C. Huang, A.D. Tward, M. J. Frederick, F. McCormick, M. Meyerson, E.M. Van Allen, A.D. Cherniack, G. Ciriello, C. Sander, N. Schultz, S.J. Caesar-Johnson, J.A. Demchok, I. Felau, M. Kasapi, M.L. Ferguson, C.M. Hutter, H.J. Sofia, R. Tarnuzzer, Z. Wang, L. Yang, J.C. Zenklusen, J. Zhang, S. Chudamani, J. Liu, L. Lolla, R. Naresh, T. Pihl, Q. Sun, Y. Wan, Y. Wu, J. Cho, T. DeFreitas, S. Frazer, N. Gehlenborg, G. Getz, D. I. Heiman, J. Kim, M.S. Lawrence, P. Lin, S. Meier, M.S. Noble, G. Saksena, D. Voet, H. Zhang, B. Bernard, N. Chambwe, V. Dhankani, T. Knijnenburg, R. Kramer, K. Leinonen, Y. Liu, M. Miller, S. Reynolds, I. Shmulevich, V. Thorsson, W. Zhang, R. Akbani, B.M. Broom, A.M. Hegde, Z. Ju, R.S. Kanchi, A. Korkut, J. Li, H. Liang, S. Ling, W. Liu, Y. Lu, G.B. Mills, K.S. Ng, A. Rao, M. Ryan, J. Wang, J.N. Weinstein, J. Zhang, A. Abeshouse, J. Armenia, D. Sofia, W.K. Chatila, I. de Bruijn, J. Gao, B.E. Gross, Z.J. Heins, R. Kundra, K. La, M. Ladanyi, A. Luna, M.G. Nissan, A. Ochoa, S.M. Phillips, E. Reznik, F. Sanchez-Vega, C. Sander, N. Schultz, R. Sheridan, S.O. Sumer, Y. Sun, B.S. Taylor, J. Wang, H. Zhang, P. Ju, M. Peto, P. Spellman, C. Benz, J.M. Stuart, C.K. Wong, C. Yau, Oncogenic signaling pathways in The Cancer Genome Atlas, Cell 173 (2018) 321–337, e10.
[41] M. Malumbres, M. Barbacid, RAS oncogenes: the first 30 years, Nat. Rev. Cancer 3 (2003) 459–465.
[42] A.G. Stephen, D. Esposito, R.K. Bagni, F. McCormick, Dragging Ras back in the ring, Cancer Cell 25 (2014) 272–281.
[43] D.K. Simanshu, D.V. Nissley, F. McCormick, RAS proteins and their regulators in human disease, Cell 170 (2017) 17–33.
[44] J.A. Engelman, Targeting PI3K signalling in cancer: opportunities, challenges and limitations, Nat. Rev. Cancer 9 (2009) 550–562.
[45] C. Kandoth, M.D. McLellan, F. Vandin, K. Ye, B. Niu, C. Lu, M. Xie, Q. Zhang, J. F. McMichael, M.A. Wyczalkowski, M.D.M. Leiserson, C.A. Miller, J.S. Welch, M. J. Walter, M.C. Wendl, T.J. Ley, R.K. Wilson, B.J. Raphael, L. Ding, Mutational landscape and significance across 12 major cancer types, Nature 502 (2013) 333–339.
[46] Y. Zhang, P. Kwok-Shing ng, M. Kucherlapati, F. Chen, Y. Liu, Y.H. Tsang, G. de Velasco, K.J. Jeong, R. Akbani, A. Hadjipanayis, A. Pantazi, C.A. Bristow, E. Lee, H.S. Mahadeshwar, J. Tang, J. Zhang, L. Yang, S. Seth, S. Lee, X. Ren, X. Song, H. Sun, J. Seidman, L.J. Luquette, R. Xi, L. Chin, A. Protopopov, T.F. Westbrook, C.S. Shelley, T.K. Choueiri, M. Ittmann, C. Van Waes, J.N. Weinstein, H. Liang, E. P. Henske, A.K. Godwin, P.J. Park, R. Kucherlapati, K.L. Scott, G.B. Mills, D. J. Kwiatkowski, C.J. Creighton, A pan-cancer proteogenomic atlas of PI3K/AKT/mTOR pathway alterations, Cancer Cell 31 (2017) 820–832, 820-832.e3.
[47] B.N. Rexer, S. Chanthaphaychith, K. Dahlman, C.L. Arteaga, Direct inhibition of PI3K in combination with dual HER2 inhibitors is required for optimal antitumor activity in HER2+ breast cancer cells, Breast Cancer Res. 16 (2014) R9.
[48] G.K. Kanev, C. de Graaf, I.J.P. de Esch, R. Leurs, T. Würdinger, B.A. Westerman, A.J. Kooistra, The landscape of atypical and eukaryotic protein kinases, Trends Pharmacol. Sci. 40 (2019) 818–832.
[49] R. Roskoski Jr., A historical overview of protein kinases and their targeted small molecule inhibitors, Pharmacol. Res. 100 (2015) 1–23.
[50] O. Vadas, J.E. Burke, X. Zhang, A. Berndt, R.L. Williams, Structural basis for activation and inhibition of class I phosphoinositide 3-kinases, Sci. Signal. 4 (195) (2011) re2.
[51] M. Zhang, H. Jang, R. Nussinov, Structural features that distinguish inactive and active PI3K lipid kinases, J. Mol. Biol. 432 (2020) 5849–5859.
[52] R. Williams, A. Berndt, S. Miller, W.C. Hon, X. Zhang, Form and flexibility in phosphoinositide 3-kinases, Biochem. Soc. Trans. 37 (2009) 615–626.
[53] A.P. Kornev, N.M. Haste, S.S. Taylor, L.F. Eyck, Surface comparison of active and inactive protein kinases identifies a conserved activation mechanism, Proc. Natl. Acad. Sci. USA 103 (2006) 17783–17788.
[54] A.P. Kornev, S.S. Taylor, Ten, L.F. Eyck, A helix scaffold for the assembly of active protein kinases, Proc. Natl. Acad. Sci. USA 105 (2008) 14377–14382.
[55] H.S. Meharena, P. Chang, M.M. Keshwani, K. Oruganty, A.K. Nene, N. Kannan, S. S. Taylor, A.P. Kornev, Deciphering the structural basis of eukaryotic protein kinase regulation, PLoS Biol. 11 (2013), e1001680.
[56] R. Roskoski Jr., Classification of small molecule protein kinase inhibitors based upon the structures of their drug-enzyme complexes, Pharmacol. Res. 103 (2016) 26–48.
[57] R. Roskoski Jr., Properties of FDA-approved small molecule protein kinase inhibitors: a 2020 update, Pharmacol. Res. 152 (2020), 104609.
[58] R. Roskoski Jr., Properties of FDA-approved small molecule protein kinase inhibitors: a 2021 update, Pharmacol. Res. 165 (2021), 105463.
[59] S. Maheshwari, M.S. Miller, R. O'Meally, R.N. Cole, L.M. Amzel, S.B. Gabelli, Kinetic and structural analyses reveal residues in phosphoinositide 3-kinase α that are critical for catalysis and substrate recognition, J. Biol. Chem. 292 (2017) 13541–13550.
[60] N. Vasan, P. Razavi, J.L. Johnson, H. Shao, H. Shah, A. Antoine, E. Ladewig, A. Gorelick, T.Y. Lin, E. Toska, G. Xu, A. Kazmi, M.T. Chang, B.S. Taylor, M. N. Dickler, K. Jhaveri, S. Chandarlapaty, R. Rabadan, E. Reznik, M.L. Smith, R. Sebra, F. Schimmoller, T.R. Wilson, L.S. Friedman, L.C. Cantley, M. Scaltriti, J. Baselga, Double PIK3CA mutations in cis increase oncogenicity and sensitivity to PI3Kα inhibitors, Science 366 (2019) 714–723.
[61] W. Cantrell, Y. Huang, A.A. Menchaca, G. Kulik, M.E. Welker, Synthesis and PI3 kinase inhibition activity of a wortmannin-leucine derivative, Molecules 23 (2018) 1791.
[62] S.E. Dalton, L. Dittus, D.A. Thomas, M.A. Convery, J. Nunes, J.T. Bush, J.P. Evans, T. Werner, M. Bantscheff, J.A. Murphy, S. Campos, Selectively targeting the kinome-conserved lysine of PI3Kδ as a general approach to covalent kinase inhibition, J. Am. Chem. Soc. 140 (2018) 932–939.
[63] J.J. Liao, Molecular recognition of protein kinase binding pockets for design of potent and selective kinase inhibitors, J. Med. Chem. 50 (2007) 409–424.
[64] O.P. van Linden, A.J. Kooistra, R. Leurs, I.J. de Esch, C. de Graaf, KLIFS: a knowledge-based structural database to navigate kinase-ligand interaction space, J. Med. Chem. 57 (2014) 249–277.
[65] G.K. Kanev, C. de Graaf, B.A. Westerman, I.J.P. de Esch, A.J. Kooistra, KLIFS: an overhaul after the first 5 years of supporting kinase research, Nucleic Acids Res. 49 (2021) D562–D569.
[66] A.J. Kooistra, A. Volkamer, Kinase-centric computational drug development, Annu. Rep. Med. Chem. 50 (2017) 197–236.
[67] D. Bajusz, G.G. Ferenczy, G.M. Keserá, Structure-based virtual screening approaches in kinase-directed drug discovery, Curr. Top. Med. Chem. 17 (2017) 2235–2259.
[68] P. Wu, T.E. Nielsen, M.H. Clausen, FDA-approved small-molecule kinase inhibitors, Trends Pharmacol. Sci. 36 (2015) 422–439.
[69] F. Carles, S. Bourg, C. Meyer, P. Bonnet, PKIDB: a curated, annotated and updated database of protein kinase inhibitors in clinical trials, Molecules 23 (4) (2018) 908, https://doi.org/10.3390/molecules23040908.
[70] R.L. Siegel, K.D. Miller, H.E. Fuchs, A. Jemal, Cancer Statistics, 2021, CA Cancer J. Clin. 71 (2021) 7–33.
[71] H. Sung, J. Ferlay, R.L. Siegel, M. Laversanne, I. Soerjomataram, A. Jemal, F. Bray, Global cancer statistics 2020: GLOBOCAN estimates of incidence and mortality worldwide for 36 cancers in 185 countries, CA Cancer J. Clin. (2021), https://doi.org/10.3322/caac.21660.

[72] J.L. Wittliff, Steroid-hormone receptors in breast cancer, Cancer 53 (1984) 630–643.
[73] P. Razavi, M.T. Chang, G. Xu, C. Bandlamudi, D.S. Ross, N. Vasan, Y. Cai, C. M. Bielski, M.T.A. Donoghue, P. Jonsson, A. Penson, R. Shen, F. Pareja, R. Kundra, S. Middha, M.L. Cheng, A. Zehir, C. Kandoth, R. Patel, K. Huberman, L. M. Smyth, K. Jhaveri, S. Modi, T.A. Traina, C. Dang, W. Zhang, B. Weigelt, B.T. Li, M. Ladanyi, D.M. Hyman, N. Schultz, M.E. Robson, C. Hudis, E. Brogi, A. Viale, L. Norton, M.N. Dickler, M.F. Berger, C.A. Iacobuzio-Donahue, S. Chandarlapaty, M. Hudis, J.S. Reis-Filho, D.B. Solit, B.S. Taylor, J. Baselga, The genomic landscape of endocrine-resistant advanced breast cancers, Cancer Cell 34 (2018) 427–438, e6.
[74] G. Fabbri, R. Dalla-Favera, The molecular pathogenesis of chronic lymphocytic leukaemia, Nat. Rev. Cancer 16 (2016) 145–162.
[75] J.A. Burger, Treatment of chronic lymphocytic leukemia, N. Engl. J. Med. 383 (2020) 460–473.
[76] R.A. de Claro, K.M. McGinn, N. Verdun, S.L. Lee, H.J. Chiu, H. Saber, M. E. Brower, C.J.G. Chang, E. Pfuma, B. Habtemariam, J. Bullock, Y. Wang, L. Nie, X.H. Chen, D. Lu, A. Al-Hakim, R.C. Kane, E. Kaminskas, R. Justice, A.T. Farrell, R. Pazdur, FDA approval: ibrutinib for patients with previously treated mantle cell lymphoma and previously treated chronic lymphocytic leukemia, Clin. Cancer Res. 21 (2015) 3586–3590.
[77] L.J. Nastoupil, C.Y. Cheah, L.J. Medeiros, N.H. Fowler, Indolent lymphomas, in: H.M. Kantarjian, R.A. Wolff (Eds.), The MD Anderson Manual of Medical Oncology, Third edition, McGraw Hill, New York, 2016, pp. 133–142.
[78] R. Roskoski Jr., Orally effective FDA-approved protein kinase targeted covalent inhibitors (TCIs), Pharmacol. Res. 165 (2021), 105422.
[79] L.J. Nastoupil, C.Y. Cheah, L.J. Medeiros, N.H. Fowler, Indolent lymphomas, in: H.M. Kantarjian, R.A. Wolff (Eds.), The MD Anderson Manual of Medical oncology, Third edition, McGraw Hill, New York, 2016, pp. 143–147.
[80] A. Sindel, T. Al-Juhaishi, V. Yazbeck, Marginal zone lymphoma: state-of-the-art treatment, Curr. Treat. Options Oncol. 20 (2019) 90.
[81] P. Furet, V. Guagnano, R.A. Fairhurst, P. Imbach-Weese, I. Bruce, M. Knapp, C. Fritsch, F. Blasco, J. Blanz, R. Aichholz, J. Hamon, D. Fabbro, G. Caravatti, Discovery of NVP-BYL719 a potent and selective phosphatidylinositol-3 kinase alpha inhibitor selected for clinical evaluation, Bioorg. Med. Chem. Lett. 23 (2013) 3741–3748.
[82] P.M. LoRusso, Inhibition of the PI3K/AKT/mTOR pathway in solid tumors, J. Clin. Oncol. 34 (2016) 3803–3815.
[83] A. Markham, Alpelisib: first global approval, Drugs 79 (2019) 1249–1253.
[84] A.J. Armaghani, H.S. Han, Alpelisib in the treatment of breast cancer: a short review on the emerging clinical data, Breast Cancer (Dove Med. Press) 12 (2020) 251–258.
[85] Z.A. Knight, B. Gonzalez, M.E. Feldman, E.R. Zunder, D.D. Goldenberg, O. Williams, R. Loewith, D. Stokoe, A. Balla, B. Toth, T. Balla, W.A. Weiss, R. L. Williams, K.M. Shokat, A pharmacological map of the PI3-K family defines a role for p110α in insulin signaling, Cell 125 (2006) 733–747.
[86] W.J. Scott, M.F. Hentemann, R.B. Rowley, C.O. Bull, S. Jenkins, A.M. Bullion, J. Johnson, A. Redman, A.H. Robbins, W. Esler, R.P. Fracasso, T. Garrison, M. Hamilton, M. Michels, J.E. Wood, D.P. Wilkie, H. Xiao, J. Levy, E. Stasik, N. Liu, M. Schaefer, M. Brands, J. Lefranc, Discovery and SAR of novel 2,3-dihydroimidazo[1,2-*c*]quinazoline PI3K inhibitors: identification of copanlisib (BAY 80-6946), ChemMedChem 11 (2016) 1517–1530.
[87] A. Eltantawy, X. Vallejos, E. Sebea, K. Evans, Copanlisib: an intravenous phosphatidylinositol 3-kinase (PI3K) inhibitor for the treatment of relapsed follicular lymphoma, Ann. Pharmacother. 53 (2019) 954–958.
[88] M. Dreyling, A. Santoro, L. Mollica, S. Leppä, G. Follows, G. Lenz, W.S. Kim, A. Nagler, M. Dimou, J. Demeter, M. Özcan, M. Kosinova, K. Bouabdallah, F. Morschhauser, D.A. Stevens, D. Trevarthen, J. Munoz, L. Rodrigues, F. Hiemeyer, A. Miriyala, J. Garcia-Vargas, B.H. Childs, P.L. Zinzani, Long-term safety and efficacy of the PI3K inhibitor copanlisib in patients with relapsed or refractory indolent lymphoma: 2-year follow-up of the CHRONOS-1 study, Am. J. Hematol. 95 (2020) 362–371, https://doi.org/10.1002/ajh.25711.
[89] P. Panayiotidis, G.A. Follows, L. Mollica, A. Nagler, M. Özcan, A. Santoro, et al., Efficacy and safety of copanlisib in patients with relapsed or refractory marginal zone lymphoma, Blood Adv. (2021) 823–828.
[90] S.E.M. Herman, A.L. Gordon, A.J. Wagner, N.A. Heerema, W. Zhao, J.M. Flynn, J. M. Flynn, J. Jones, L. Andritsos, K.D. Puri, B.J. Lannutti, N.A. Giese, X. Zhang, L. Wei, J.C. Byrd, A.J. Johnson, Phosphatidylinositol 3-kinase-δ inhibitor CAL-101 shows promising preclinical activity in chronic lymphocytic leukemia by antagonizing intrinsic and extrinsic cellular survival signals, Blood 116 (2010) 2078–2088.
[91] C.Y. Cheah, N.H. Fowler, Idelalisib in the management of lymphoma, Blood 128 (2016) 331–336.
[92] B.J. Lannutti, S.A. Meadows, S.E.M. Herman, A. Kashishian, B. Steiner, A. J. Johnson, J.C. Byrd, J.W. Tyner, M.M. Loriaux, M. Deininger, B.J. Druker, K. D. Puri, R.G. Ulrich, N.A. Giese, CAL-101, a p110δ selective phosphatidylinositol-3-kinase inhibitor for the treatment of B-cell malignancies, inhibits PI3K signaling and cellular viability, Blood 117 (2011) 591–594.
[93] Q. Yang, P. Modi, T. Newcomb, C. Quéva, V. Gandhi, Idelalisib: first-in-class PI3K delta inhibitor for the treatment of chronic lymphocytic leukemia, small lymphocytic leukemia, and follicular lymphoma, Clin. Cancer Res. 21 (2015) 1537–1542.
[94] D.G. Winkler, K.L. Faia, J.P. DiNitto, J.A. Ali, K.F. White, E.E. Brophy, M.M. Pink, J.L. Proctor, J. Lussier, C.M. Martin, J.G. Hoyt, B. Tillotson, E.L. Murphy, A. R. Lim, B.D. Thomas, J.R. MacDougall, P. Ren, Y. Liu, L.S. Li, K.A. Jessen, C. C. Fritz, J.L. Dunbar, J.R. Porter, C. Rommel, V.J. Palombella, P.S. Changelian, J. L. Kutok, PI3K-δ and PI3K-γ inhibition by IPI-145 abrogates immune responses and suppresses activity in autoimmune and inflammatory disease models, Chem. Biol. 20 (2013) 1364–1374.
[95] M. Spaargaren, E.A. Beuling, M.L. Rurup, H.P. Meijer, M.D. Klok, S. Middendorp, R.W. Hendriks, S.T. Pals, The B cell antigen receptor controls integrin activity through Btk and PLCγ2, J. Exp. Med. 198 (2003) 1539–1550.
[96] K. Balakrishnan, M. Peluso, M. Fu, N.Y. Rosin, J.A. Burger, W.G. Wierda, M. J. Keating, K. Faia, S. O'Brien, J.L. Kutok, V. Gandhi, The phosphoinositide-3-kinase (PI3K)-delta and gamma inhibitor, IPI-145 (duvelisib), overcomes signals from the PI3K/AKT/S6 pathway and promotes apoptosis in CLL, Leukemia 29 (2015) 1811–1822.
[97] S. Dong, D. Guinn, J.A. Dubovsky, Y. Zhong, A. Lehman, J. Kutok, J.A. Woyach, J. C. Byrd, A.J. Johnson, IPI-145 antagonizes intrinsic and extrinsic survival signals in chronic lymphocytic leukemia cells, Blood 124 (2014) 3583–3586.
[98] H.A. Blair, Duvelisib: first global approval, Drugs 78 (2018) 1847–1853.
[99] B.L. Lampson, J.R. Brown, PI3Kδ-selective and PI3Kα/δ-combinatorial inhibitors in clinical development for B-cell non-Hodgkin lymphoma, Expert Opin. Investig. Drugs 26 (2017) 1267–1279.
[100] C. Deng, M.R. Lipstein, L. Scotto, X.O. Jirau Serrano, M.A. Mangone, S. Li, J. Vendome, Y. Hao, X. Xu, S.X. Deng, R.B. Realubit, N.P. Tatonetti, C. Karan, S. Lentzsch, D.A. Fruman, B. Honig, D.W. Landry, O.A. O'Connor, Silencing c-Myc translation as a therapeutic strategy through targeting PI3Kδ and CK1ε in hematological malignancies, Blood 129 (2017) 88–99.
[101] G. von Keudell, A.J. Moskowitz, The role of PI3K inhibition in lymphoid malignancies, Curr. Hematol. Malig. Rep. 14 (5) (2019) 405–413.
[102] H.A. Burris 3rd, I.W. Flinn, M.R. Patel, T.S. Fenske, C. Deng, D.M. Brander, M. Gutierrez, J.H. Essell, J.G. Kuhn, H.P. Miskin, P. Sportelli, M.S. Weiss, S. Vakkalanka, M.R. Savona, O.A. O'Connor, Umbralisib, a novel PI3Kδ and casein kinase-1ε inhibitor, in relapsed or refractory chronic lymphocytic leukaemia and lymphoma: an open-label, phase 1, dose-escalation, first-in-human study, Lancet Oncol. 19 (2018) 486–496.
[103] C.A. Lipinski, F. Lombardo, B.W. Dominy, P.J. Feeney, Experimental and computational approaches to estimate solubility and permeability in drug discovery and development settings, Adv. Drug Deliv. Rev. 46 (2001) 3–26.
[104] A.L. Hopkins, C.R. Groom, A. Alex, Ligand efficiency: a useful metric for lead selection, Drug Discov. Today 9 (2004) 430–431.
[105] G.F. Smith, Medicinal chemistry by the numbers: the physicochemistry, thermodynamics and kinetics of modern drug design, Prog. Med. Chem. 48 (2009) 1–29.
[106] P.D. Leeson, B. Springthorpe, The influence of drug-like concepts on decision-making in medicinal chemistry, Nat. Rev. Drug Discov. 6 (2007) 881–890.
[107] S. Ekins, N.K. Litterman, C.A. Lipinski, B.A. Bunin, Thermodynamic proxies to compensate for biases in drug discovery methods, Pharm. Res. 33 (2016) 194–205.
[108] A.L. Hopkins, G.M. Keserü, P.D. Leeson, D.C. Rees, C.H. Reynolds, The role of ligand efficiency metrics in drug discovery, Nat. Rev. Drug Discov. 13 (2014) 105–121.
[109] P.D. Leeson, Molecular inflation, attrition, and the rule of five, Adv. Drug Deliv. Rev. 101 (2016) 22–33.
[110] D.F. Veber, S.R. Johnson, H.Y. Cheng, B.R. Smith, K.W. Ward, K.D. Kopple, Molecular properties that influence the oral bioavailability of drug candidates, J. Med. Chem. 45 (2002) 2615–2623.
[111] J.J. Cui, M. Tran-Dubé, H. Shen, M. Nambu, P.P. Kung, M. Pairish, L. Jia, J. Meng, L. Funk, I. Botrous, M. McTigue, N. Grodsky, K. Ryan, E. Padrique, G. Alton, S. Timofeevski, S. Yamazaki, Q. Li, H. Zou, J. Christensen, B. Mroczkowski, S. Bender, R.S. Kania, M.P. Edwards, Structure based drug design of crizotinib (PF-02341066), a potent and selective dual inhibitor of mesenchymal-epithelial transition factor (c-MET) kinase and anaplastic lymphoma kinase (ALK), J. Med. Chem. 54 (2011) 6342–6363.
[112] R. Roskoski Jr., Anaplastic lymphoma kinase (ALK): structure, oncogenic activation, and pharmacological inhibition, Pharmacol. Res. 68 (2013) 68–94.
[113] R. Roskoski Jr., The preclinical profile of crizotinib in the treatment of non-small cell lung cancer and other neoplastic disorders, Expert Opin. Drug Discov. 8 (2013) 1165–1179.
[114] R. Roskoski Jr., Anaplastic lymphoma kinase (ALK) inhibitors in the treatment of ALK-driven lung cancers, Pharmacol. Res. 117 (2017) 343–356.
[115] T.I. Oprea, Property distribution of drug-related chemical databases, J. Comput. Aided Mol. Des. 14 (2000) 251–264.
[116] S.H. Bertz, The first general index of molecular complexity, J. Am. Chem. Soc. 1103 (1981) 3559–3601.
[117] J.B. Hendrickson, P. Huang, A.G. Toczko, Molecular complexity: a simplified formula adapted to individual atoms, J. Chem. Inf. Comput. Sci. 27 (1987) 63–67.
[118] A. Inui, Cancer anorexia-cachexia syndrome: are neuropeptides the key? Cancer Res. 59 (1999) 4493–4501.
[119] M. Reinwald, J.T. Silva, N.J. Mueller, J. Fortún, C. Garzoni, J.W. de Fijter, M. Fernández-Ruiz, P. Grossi, J.M. Aguado, ESCMID Study Group for Infections in Compromised Hosts (ESGICH) consensus document on the safety of targeted and biological therapies: an infectious diseases perspective (intracellular signaling pathways: tyrosine kinase and mTOR inhibitors), Clin. Microbiol. Infect. 24 (Suppl. 2) (2018) S53–S70.
[120] X.Z. Shi, S.K. Sarna, G protein-mediated dysfunction of excitation-contraction coupling in ileal inflammation, Am. J. Physiol. Gastrointest. Liver Physiol. 286 (2004) G899–G905.
[121] G. Maschmeyer, J. De Greef, S.C. Mellinghoff, A. Nosari, A. Thiebaut-Bertrand, A. Bergeron, et al., Infections associated with immunotherapeutic and molecular

targeted agents in hematology and oncology. A position paper by the European Conference on Infections in Leukemia (ECIL), Leukemia 33 (2019) 844–862.
[122] Z. Xie, X. Yang, Y. Duan, J. Han, C. Liao, Small-molecule kinase inhibitors for the treatment of nononcologic diseases, J. Med. Chem. 64 (2021) 1283–1345.
[123] B.S. Kahl, S.E. Spurgeon, R.R. Furman, I.W. Flinn, S.E. Coutre, J.R. Brown, D. M. Benson, J.C. Byrd, S. Peterman, Y. Cho, A. Yu, W.R. Godfrey, N.D. Wagner-Johnston, A phase 1 study of the PI3Kδ inhibitor idelalisib in patients with relapsed/refractory mantle cell lymphoma (MCL), Blood 123 (2014) 3398–3405.
[124] J. Rodon, R. Dienstmann, V. Serra, J. Tabernero, Development of PI3K inhibitors: lessons learned from early clinical trials, Nat. Rev. Clin. Oncol. 10 (2013) 143–153.
[125] E. Van Cutsem, S. Tejpar, D. Vanbeckevoort, M. Peeters, Y. Humblet, H. Gelderblom, J.B. Vermorken, F. Viret, B. Glimelius, E. Gallerani, A. Hendlisz, A. Cats, M. Moehler, X. Sagaert, S. Vlassak, M. Schlichting, F. Ciardiello, Intrapatient cetuximab dose escalation in metastatic colorectal cancer according to the grade of early skin reactions: the randomized EVEREST study, J. Clin. Oncol. 30 (2012) 2861–2868.
[126] B.D. Hopkins, M.D. Goncalves, L.C. Cantley, Insulin-PI3K signalling: an evolutionarily insulated metabolic driver of cancer, Nat. Rev. Endocrinol. 16 (2020) 276–283.
[127] B.D. Hopkins, C. Pauli, X. Du, D.G. Wang, X. Li, D. Wu, S.C. Amadiume, M. D. Goncalves, C. Hodakoski, M.R. Lundquist, R. Bareja, Y. Ma, E.M. Harris, A. Sboner, H. Beltran, M.A. Rubin, S. Mukherjee, L.C. Cantley, Suppression of insulin feedback enhances the efficacy of PI3K inhibitors, Nature 560 (2018) 499–503.
[128] R. Roskoski Jr., Guidelines for preparing color figures for everyone including the colorblind, Pharmacol. Res. 119 (2017) 240–241. Erratum in: Pharmacol. Res. 2019; 139: 569.